

1 ~~Export fluxes in a naturally fertilized area of the Southern Ocean,~~
2 ~~the Kerguelen Plateau: seasonal dynamic reveals long lags and~~
3 ~~strong attenuation of particulate organic carbon flux (part 1).~~

4 **Export fluxes in a naturally iron-fertilized area of the Southern**
5 **Ocean: seasonal dynamics of particulate organic carbon export**
6 **from a moored sediment trap (part 1).**

7
8 M. Rembauville^{1,2}, I. Salter^{1,2,3}, N. Leblond^{4,5}, A. Gueneugues^{1,2} and S. Blain^{1,2}

9 ¹ Sorbonne Universités, UPMC Univ Paris 06, UMR 7621, LOMIC, Observatoire Océanologique, Banyuls-sur-Mer, France.

10
11 ² CNRS, UMR 7621, LOMIC, Observatoire Océanologique, Banyuls-sur-Mer, France.

12
13 ³ Alfred-Wegener-Institute for Polar and Marine research, Bremerhaven, Germany.

14
15 ⁴ Sorbonne Universités, UPMC Univ Paris 06, LOV, UMR 7093, Observatoire Océanologique, Villefranche-sur-Mer, France

16
17 ⁵ CNRS-INSU, LOV, UMR 7093, Observatoire Océanologique, Villefranche-sur-Mer, France

18
19
20 Correspondance to: M. Rembauville (rembauville@obs-banyuls.fr).

21
22
23 **Abstract**

24
25 A sediment trap moored in the naturally iron-fertilized Kerguelen plateau in the Southern
26 Ocean provided an annual record of particulate organic carbon and nitrogen fluxes at 289 m.
27 At the trap deployment depth current speeds were typically low ($\sim 10 \text{ cm s}^{-1}$) and primarily
28 tidal-driven (M2 tidal component). ~~providing favorable hydrodynamic conditions for the~~
29 ~~collection of flux.~~ Although advection was weak, the sediment trap may have been subject to
30 hydrodynamical and biological (swimmer feeding on trap funnel) biases that could explain the

31 collection of only 15-30 % of the ²³⁴Th derived flux. Particulate organic carbon (POC) flux
32 was generally low (<0.5 mmol m⁻² d⁻¹) although two episodic export events (<14 days) of 1.5
33 mmol m⁻² d⁻¹ were recorded. These increases in flux occurred with a 1-month time lag from
34 peaks in surface chlorophyll and together accounted for approximately 40 % of the annual
35 flux budget. The annual POC flux of 98.2±4.4 mmol m⁻² y⁻¹ was low considering the shallow
36 deployment depth, but comparable to independent estimates made at similar depths (~300m)
37 over the plateau and to deep-ocean (>2 km) fluxes measured from similarly productive iron-
38 fertilized blooms. Although undertrapping cannot be excluded in shallow moored sediment
39 trap deployment, we hypothesize that grazing pressure, including mesozooplankton and
40 mesopelagic fishes, may be responsible for the large reduction in POC flux beneath the base
41 of the winter mixed layer. The importance of plankton community structure in controlling the
42 temporal variability of export fluxes is addressed in a companion paper.

43

44 **1 Introduction**

45 The biological carbon pump is defined as the vertical transfer of biologically fixed
46 carbon in the ocean surface to the ocean interior (Volk and Hoffert, 1985). Global estimates of
47 Particulate Organic Carbon (POC) export cluster between 5 Pg C y⁻¹ (Moore et al., 2004; Lutz
48 et al., 2007; Honjo et al., 2008; Henson et al., 2011; Lima et al., 2014a) to 10 Pg C y⁻¹ (Laws
49 et al., 2000; Schlitzer, 2004; Gehlen et al., 2006; Boyd and Trull, 2007; Dunne et al., 2007;
50 Laws et al., 2011). ~~Nevertheless~~ The physical transfer of dissolved inorganic carbon to the
51 ocean interior during subduction of water masses is two orders of magnitude higher (> 250 Pg
52 C y⁻¹, Karleskind et al., 2011; Levy et al., 2013). The global ocean represents a net annual
53 CO₂ sink of 2.5 Pg C y⁻¹ (Le Quéré et al., 2013), slowing down the increase of the
54 atmospheric CO₂ concentration resulting from anthropogenic activity. Although the Southern
55 Ocean (south of 44°S) plays a limited role in the net air-sea CO₂ flux (Lenton et al., 2013), it
56 is a key component of the global anthropogenic CO₂ sink representing one third the global
57 oceanic sink (~1 Pg C y⁻¹) while covering 20 % of its surface (Gruber et al., 2009). The
58 solubility pump is considered as the major component of this sink, ~~whereas the biological~~
59 ~~carbon pump is considered to be inefficient in the Southern Ocean and sensitive to iron~~
60 ~~supply.~~

61 Following “~~the iron hypothesis~~” in the nineties (Martin 1990), iron limitation of high
62 nutrient low chlorophyll (HNLC) areas, including the Southern Ocean, has been tested in
63 bottle experiments (de Baar et al., 1990) and through *in situ* artificial fertilization experiments
64 (de Baar et al., 2005; Boyd et al., 2007). Results from these experiments are numerous and
65 essentially highlight that iron limits macronutrient (N, P, Si) utilization (Boyd et al., 2005;
66 Hiscock and Millero, 2005) and primary production (Landry et al., 2000; Gall et al., 2001;
67 Coale et al., 2004) in these vast HNLC areas of the Southern Ocean. Due to a large
68 macronutrient repository the biological carbon pump in the Southern Ocean is considered to

69 be inefficient in its capacity to transfer atmospheric carbon to the ocean interior (Sarmiento
70 and Gruber, 2006). In the context of micronutrient limitation, sites enriched in iron by natural
71 processes have also been studied and include the Kerguelen islands (Blain et al., 2001, 2007),
72 the Crozet islands (Pollard et al., 2007), the Scotia Sea (Tarling et al., 2012), and the Drake
73 Passage (Measures et al., 2013). Enhanced primary producer biomass in association with
74 natural iron supply (Korb and Whitehouse, 2004; Seeyave et al., 2007; Lefèvre et al., 2008)
75 strongly support trace-metal limitation. Furthermore, indirect seasonal budgets constructed
76 from studies of naturally fertilized systems have been capable of demonstrating an increase in
77 the strength of the biological carbon pump (Blain et al., 2007; Pollard et al., 2009), although
78 strong discrepancies in carbon to iron sequestration efficiency exist between systems. To date,
79 direct measurements of POC export from naturally fertilized blooms in the Southern Ocean
80 are limited to the Crozet Plateau (Pollard et al., 2009; Salter et al., 2012). The HNLC
81 Southern Ocean represents a region where changes in the strength of the biological pump may
82 have played a role in the glacial-interglacial CO₂ cycles (Bopp et al., 2003; Kohfeld et al.,
83 2005) and have some significance to future anthropogenic CO₂ uptake (Sarmiento and Le
84 Quéré, 1996). In this context, additional studies that directly measure POC export from
85 naturally iron-fertilized blooms in the Southern Ocean are necessary.

86 POC export can be estimated at short timescales (days to weeks) using the ²³⁴Th proxy
87 (Coale and Bruland, 1985; Buesseler et al., 2006; Savoye et al., 2006), by optical imaging of
88 particles (e.g. Picheral et al., 2010) or by directly collecting particles into surface-tethered
89 sediment traps (e.g. Maiti et al., 2013 for a compilation in the Southern Ocean) or neutrally
90 buoyant sediment traps (e.g. Salter et al., 2007; Rynearson et al., 2013). Temporal variability
91 of flux in the Southern Ocean precludes extrapolation of discrete measurements to estimate
92 seasonal or annual carbon export. However seasonal export of POC can be derived from
93 biogeochemical budgets (Blain et al., 2007; Pollard et al., 2009) or be directly measured by

94 moored sediment traps (e.g. Salter et al., 2012). Biogeochemical budgets are capable of
95 integrating over large spatial and temporal scales but may incorporate certain assumptions and
96 lack information about underlying mechanisms. Direct measurement by sediment traps rely
97 on fewer assumptions but their performance is strongly related to prevailing hydrodynamic
98 conditions (Buesseler et al., 2007a), which can be particularly problematic in the surface
99 ocean. Measuring the hydrological conditions characterizing mooring deployments is
100 ~~necessary therefore crucial~~ to address issues surrounding the efficiency of sediment trap
101 collection.

102 The ecological processes responsible for carbon export remain poorly characterized
103 (Boyd and Trull, 2007). ~~Having direct access to the exported material in a quantitative way~~
104 ~~There is a strong requirement for quantitative analysis of the biological components of export~~
105 ~~to~~ elucidate patterns in carbon and biomineral fluxes to the ocean interior (Francois et al.,
106 2002; Salter et al., 2010; Henson et al., 2012; Le Moigne et al., 2012; Lima et al., 2014).
107 Long-term deployment of moored sediment traps in areas of naturally iron fertilized
108 production, where significant macro- and micro-nutrient gradients seasonally structure
109 plankton communities, can help to establish links between ecological succession and carbon
110 export. For example, sediment traps around the Crozet Plateau (Pollard et al., 2009) identified
111 the significance of *Eucampia antarctica* var. *antarctica* resting spores for carbon transfer to
112 the deep ocean, large empty diatom frustules for Si:C export stoichiometry (Salter et al.,
113 2012), and heterotrophic calcifiers for the carbonate counter pump (Salter et al., 2014).

114 The increase in primary production resulting from natural fertilization might not
115 necessarily lead to significant increases in carbon export. The concept of “High Biomass, Low
116 Export” (HBLE) environments was first introduced in the Southern Ocean (Lam and Bishop,
117 2007). This concept is partly based on the idea that a strong grazer response to phytoplankton
118 biomass leads to major fragmentation and remineralization of particles in the twilight zone,

119 shallowing the remineralization horizon (Coale et al., 2004). ~~Alternative explanations suggest~~
120 ~~that~~ **In these environments**, the efficient utilization and reprocessing of exported carbon by
121 zooplankton leads to fecal pellet dominated, low POC fluxes (Ebersbach et al., 2011). A
122 synthesis of short-term sediment trap deployments, ²³⁴Th estimates of upper ocean POC
123 export and in situ primary production measurements in the Southern Ocean by Maiti et al.
124 (2013) has highlighted the inverse relationship between primary production and export
125 efficiency, verifying the HBLE status of many productive areas in the Southern Ocean. The
126 iron fertilized bloom above the Kerguelen Plateau exhibits strong remineralization in the
127 mixed layer compared to the mesopelagic, (Jacquet et al., 2008) and high bacterial carbon
128 demand (Obenosterer et al., 2008), features consistent with a HBLE regime. Moreover, an
129 inverse relationship between export efficiency and zooplankton biomass in the Kerguelen
130 Plateau region support the key role of grazers in the HBLE scenario (Laurenceau et al., 2014).
131 Efficient grazer responses to phytoplankton biomass following artificial iron fertilization of
132 HNLC regions also demonstrate increases in net community production that are not translated
133 to an increase in export fluxes (Lam and Bishop, 2007; **Tsuda et al., 2007**; Martin et al., 2013;
134 Batten and Gower, 2014).

135 POC flux attenuation with depth results from processes occurring in the euphotic layer
136 (setting the particle export efficiency, Henson et al., 2012) and processes occurring in the
137 twilight zone between the euphotic layer and ~1000 m (Buesseler and Boyd, 2009), setting
138 the transfer efficiency (Francois et al., 2002). These processes are mainly biologically-driven
139 (Boyd and Trull, 2007) and involve a large diversity of ecosystem components from bacteria
140 (Rivkin and Legendre, 2001; Giering et al., 2014), protozooplankton (Barbeau et al., 1996),
141 mesozooplankton (Dilling and Alldredge, 2000; Smetacek et al., 2004) and mesopelagic
142 fishes (Davison et al., 2013; Hudson et al., 2014). The net effect **of** these processes is
143 summarized in a power-law formulation of POC flux attenuation with depth proposed by

144 Martin et al. (1987) that is still commonly used in data and model applications. The b-
145 exponent in this formulation has been reported to range from 0.4 to 1.7 (Buesseler et al.,
146 2007b; Lampitt et al., 2008; Henson et al., 2012) in the global Ocean. Nevertheless, a change
147 in the upper mesopelagic community structure (Lam et al., 2011), and more precisely an
148 increasing contribution of mesozooplankton (Lam and Bishop, 2007; Ebersbach et al., 2011)
149 could lead to a shift toward higher POC flux attenuation with depth.

150 In this paper, we provide the first annual description of the POC and PON export
151 fluxes below the mixed layer within the naturally fertilized bloom of the Kerguelen Plateau
152 and we discuss the reliability of these measurements considering the hydrological and
153 biological context. A companion paper (Rembauville et al., 2014) addresses our final aim: to
154 identify the ecological vectors that explain the intensity and the stoichiometry of the fluxes.

155 **2 Material and Methods**

156 **2.1 Trap deployment and mooring design**

157 As part of the KEOPS2 multidisciplinary program, a mooring line was deployed at
158 station A3 (50°38.3 S – 72°02.6 E) in the Permanently Open Ocean Zone (POOZ), south of
159 the Polar Front (PF) (Fig. 1). The mooring line was instrumented with a Technicap PPS3
160 (0.125 m² collecting area, 4.75 aspect ratio) sediment trap and inclinometer (NKE S2IP) at a
161 depth of 289 m (seafloor depth 527 m) (Fig. 2). A conductivity-temperature-pressure (CTD)
162 sensor (Seabird SBE 37) and a current meter (Nortek Aquadopp) were placed on the mooring
163 line 30 m beneath the sediment trap (319 m). The sediment trap collection period started on
164 21 October 2011 until 7 September 2012. The sediment trap was composed of twelve rotating
165 sample cups (250 mL) filled with a 5 % formalin hypersaline solution buffered with sodium
166 tetraborate at pH = 8. Rotation of the carousel was programmed to sample short intervals (10-
167 14 days) between October and February, to optimize the temporal resolution of export from
168 the bloom, and long intervals (99 days) between February and September. All instruments had
169 a 1 hour recording interval. The current meter failed on the 7th April 2012.

170 **2.3 Surface chlorophyll data**

171 The MODIS AQUA level 3 (4 km grid resolution, 8 day averages) surface chlorophyll
172 *a* product was extracted from the NASA website (<http://oceancolor.gsfc.nasa.gov/>) for
173 sediment trap deployment period. An annual climatology of surface chlorophyll *a*
174 concentration, based on available satellite products (1997-2013), was calculated from the
175 multisatellite Globcolour product. The Globcolour level 3, (case 1 waters, 4.63 km resolution,
176 8 day averages) product merging Seawifs, MODIS and MERIS data with GSM merging
177 model (Maritorena and Siegel, 2005) was accessed via <http://www.globcolour.info>. Surface
178 chlorophyll *a* concentrations derived from Globcolour (climatology) and MODIS data

179 (deployment year) were averaged across a 100 km radius centered on the sediment trap
180 deployment location (Fig. 1).

181 **2.3 Time series analyses of hydrological parameters**

182 Fast Fourier Transform (FFT) analysis was performed on the annual time series data obtained
183 from the mooring, depth and potential density anomaly (σ_θ) that were derived from the CTD
184 sensor. Significant peaks in the power spectrum were identified by comparison to red noise, a
185 theoretical signal in which the relative variance decreases with increasing frequency (Gilman
186 et al., 1963). The red noise signal was considered as a null hypothesis and its power spectrum
187 was scaled to the 99th percentile of χ^2 probability. Power peaks higher than 99 % red noise
188 values were considered to be statistically significant (Schulz and Mudelsee, 2002), enabling
189 the identification of periods of major variability in time series. In order to identify the water
190 masses surrounding the trap, temperature and salinity recorded by the mooring CTD were
191 placed in context to previous CTD casts conducted at A3 during KEOPS1 (39 profiles, 23
192 January 2005 - 13 February 2005) and KEOPS2 (12 profiles, from 15 - 17 November).

193 **2.4 Sediment trap material analyses**

194 Upon recovery of the sediment trap the pH of the supernatant was measured **in every cup** and
195 1 mL of 37 % formalin buffered with sodium tetraborate (pH=8) **was added**. After allowing
196 the particulate material to settle to the base of the sample cup (~24 hrs), 60 mL of supernatant
197 was removed with a syringe and stored separately. The samples were transported in the dark
198 at 4°C (JGOFS Sediment Trap Methods, 1994) and stored under identical conditions upon
199 arrival at the laboratory until further analysis. Nitrate, nitrite, ammonium and phosphate in the
200 **withdrawn** supernatant were analysed colorimetrically (Aminot and Kerouel, 2007) to check
201 for possible leaching of dissolved inorganic nitrogen and phosphorus from the particulate
202 phase.

203 Samples were first transferred ~~in~~ to a petri dish and examined under stereomicroscope
204 (Leica MZ8, x10 to x50 magnification) to determine and isolate swimmers (i.e. organisms
205 that actively entered the cup). All swimmers were carefully sorted, cleaned (rinsed with
206 preservative solution), enumerated and removed from the cups for further taxonomic
207 identification. ~~As the~~ The classification of organisms as swimmers remains subjective and
208 there is no standardized protocol. We classified zooplankton organisms as swimmers if we
209 ~~could observe~~ organic material and preserved structures ~~could be observed~~. Empty shells,
210 exuvia (exoskeleton remains) and organic debris were considered part of the passive flux.
211 Sample preservation prevented the identification of smaller swimmers (mainly copepods) but,
212 where possible, zooplankton were identified following Boltovskoy (1999).

213 Following the removal of swimmers, samples were quantitatively split into eight
214 aliquots using a Jencons peristaltic splitter. A splitting precision of 2.9 % (coefficient of
215 variation) was determined by weighing the particulate material obtained from each of four
216 1/8th aliquots (see below). Aliquots for chemical analyses were centrifuged (5 min at 3000
217 rpm) with the supernatant being withdrawn after this step and replaced by milliQ-grade water
218 to remove salts (~~Milli-Q rinses were compared with ammonium formate. Organic carbon~~
219 ~~content was not statistically different although nitrogen concentrations were significantly~~
220 ~~higher, consequently Milli-Q rinses were routinely performed~~). ~~This~~ The rinsing step was
221 repeated three times. The remaining pellet was freeze-dried (SGD-SERAIL, 0.05-0.1 mbar, -
222 30 °C to 30 °C, 48h run) and weighed three times (Sartorius MC 210 P balance, precision 10⁻⁴
223 g) to calculate the total mass. The particulate material was ground to a fine powder and used
224 for measurements of particulate constituents.

225 For particulate organic carbon (POC) and particulate organic nitrogen (PON) analyses,
226 3 to 5 mg of the freeze-dried powder was weighed directly into pre-combusted (450°C, 24h)
227 silver cups. Samples were decarbonated by adding 20 µL of 2M analytical grade Hydrochloric

228 acid (Sigma-Aldrich). Acidification was repeated until no bubbles could be seen, ensuring all
229 particulate carbonate was dissolved (Salter et al., 2010). Samples were dried overnight at 50
230 °C. POC and PON were measured with a CHN analyzer (Perkin Elmer 2400 Series II
231 CHNS/O Elemental Analyzer) calibrated with glycine. Samples were analysed in triplicate
232 with an analytical precision of less than 0.7 %. Due to the small amount of particulate
233 material in sample cups #5 and #12, replicate analyses were not possible. Uncertainty
234 propagation for POC and PON flux was calculated as the quadratic sum of errors on mass flux
235 and POC/PON content in each sample. The annual flux (\pm standard deviation) was calculated
236 as the sum of the time-integrated flux (~~\pm standard deviation) in each cup.~~

237 ~~In addition, transmissiometer (Wetlabs C star) profiles from the KEOPS2 cruise were~~
238 ~~used to estimate POC profiles. The transmissiometer signal was calibrated against POC data~~
239 ~~(Lasbleiz et al., 2014) with the following equation: $POC (\mu M) = \log(X_{miss}/100) * -100.74 +$~~
240 ~~0.6401 .~~

241 3. Results

242 3.1 Physical conditions around trap

243 The sediment trap was deployed in the upper layers of Upper Circumpolar Deep Water
244 (UCDW), beneath seasonally mixed Winter Water (WW) (Fig. 2). The depth of the CTD
245 sensor varied between 318 m and 322 m (1 % and 99 % quantiles), with rare deepening to 328
246 m (Fig. 3a). Variations in tilt angle of the sediment trap were also low, mostly between 1 °
247 and 5 °, and occasionally reaching 13 ° (Fig. 3d). Current speed amplitude varied between 4
248 cm s⁻¹ and 23 cm s⁻¹ (1 % and 99 % quantiles) with a maximum value of 33 cm s⁻¹ and a mean
249 value of 9 cm s⁻¹ (Fig. 3e). Horizontal flow vectors were divided between northward and
250 southward components with strongest current speeds observed to flow northward (Fig. 3f and
251 3g).

252 The range in potential temperature and salinity was 1.85–2.23 °C and 34.12 – 34.26 (1
253 % - 99 % quantiles) (Fig. 3b and 3c). From July to September 2012, a mean increase of 0.2°C
254 in potential temperature was associated with a strong diminution of high frequency noise
255 suggesting a drift of the temperature sensor. Consequently these temperature data were
256 rejected from the time-series analysis. The potential temperature/salinity diagram is compared
257 to KEOPS1 and KEOPS2 CTD downcast at station A3 (Fig. 4). The CTD sensor recorded the
258 signature of the UCDW and no intrusion of overlying WW could be detected.

259 The power spectrum of vertical sediment trap displacements identified six significant
260 peaks corresponding to frequencies of 6.2 h, 8.2 h, 23.9 h, 25.7 h and 14 days (Fig 5a).
261 Concomitant peaks of depth, angle and current speed were also observed with a period of 14
262 days. However, spectral analysis of the potential density anomaly σ_θ revealed only one
263 significant major power peak corresponding to a frequency of 12.4 h (Fig. 5b). Isopycnal
264 displacements were driven by the unique tidal component (M2, 12.4h period) and trap
265 displacements resulted from a complex combination of multiple tidal components. The power
266 spectrum analysis suggested that a 40 hour window was relevant to filter out most of the short
267 term variability (black line in Fig 3a – 3e).

268 A pseudo-lagrangian trajectory was calculated by cumulating the instantaneous current
269 vectors (Fig 6). Over short time-scales (hours to day) the trajectory displays numerous tidal
270 ellipses. The flow direction is mainly to the South-East in October 2011 to December 2012
271 and North-East from December 2011 to April 2012. For the entire current meter record (6
272 months) the overall displacement followed a 120 km northeasterly, anticlockwise trajectory
273 with an integrated current speed of approximately 1 cm s⁻¹.

274 **3.2 Seasonality of surface chlorophyll *a* concentration above trap location**

275 The seasonal variations of surface chlorophyll *a* concentration for the sediment trap
276 deployment period differed significantly from the long-term climatology (Fig 7a). The bloom
277 started at the beginning of November 2011, ten days after the start of the sediment trap
278 deployment. Maximum surface chlorophyll *a* values of 2.5 $\mu\text{g L}^{-1}$ occurred on the first week
279 of November and subsequently declined rapidly to 0.2 $\mu\text{g L}^{-1}$ in late December 2011. A
280 second increase in surface chlorophyll *a* up to 1 $\mu\text{g L}^{-1}$ occurred in January 2012 and values
281 decreased to winter levels of 0.2 $\mu\text{g L}^{-1}$ in February 2012. A short-term increase of 0.8 $\mu\text{g L}^{-1}$
282 occurred in mid-April 2012.

283 **3.3 Swimmer abundances**

284 No swimmers were found in cups #3 and #5 (Table 2). Total swimmer numbers were highest
285 in winter (1544 individuals in cup #12). When normalized to cup opening time, swimmer
286 intrusion rates were highest between mid-December 2011 and mid-February 2012 (from 26 to
287 55 individuals d^{-1}) and lower than 20 individuals d^{-1} for the remainder of the year. Swimmers
288 were numerically dominated by copepods throughout the year, but elevated amphipod and
289 pteropod abundances were observed at the end of January and February 2012 (Table 2). There
290 was no significant correlation between mass flux, POC and PON fluxes and total swimmer
291 number or intrusion rate (Spearman's correlation test, $p > 0,01$). Copepods were essentially
292 small cyclopoid species. Amphipods were predominantly represented by the hyperidean
293 *Cylopus magellanicus* and *Themisto gaudichaudii*. Pteropods were represented by *Clio*
294 *pyramidata*, *Limacina helicina* forma *antarctica* and *Limacina retroversa* subsp. *australis*.
295 Euphausiids were only represented by the genus *Thysanoessa*. One *Slapa thompsoni* salp
296 (aggregate form) was found in the last winter cup #12.

297 **3.4 Seasonal particulate organic carbon and nitrogen fluxes**

298 Particulate organic carbon flux ranged from 0.15 to 0.55 mmol m⁻² d⁻¹ during the productive
299 period except during two short export events of 1.6 ± 0.04 and 1.5 ± 0.04 mmol m⁻² d⁻¹
300 sampled in cups #4 (2 to 12 December 2011) and #9 (25 January to 8 February 2012),
301 respectively (Fig. 7b). The two flux events occurred with an approximate time lag of one
302 month compared to peaks in surface chlorophyll *a* values. A modest value of 0.27±0.01 mmol
303 m⁻² d⁻¹ was observed in autumn (cup #11, 22 February to 30 May 2012). The lowest POC flux
304 was measured during winter (0.04 mmol m⁻² d⁻¹, cup #12, 31 May to 7 October). Assuming
305 that POC export was negligible from mid September to mid October, the annually integrated
306 POC flux was 98.2 ± 4.4 mmol m⁻² y⁻¹ (Table 1). The two short (<14 days) export events
307 accounted for 16.2±0.5 % (cup #4) and 21.0±0.6 % (cup #9) of the annual carbon export out
308 of the mixed layer (Table 1). Mass percentage of organic carbon ranged from 3.3 % to 17.4 %
309 (Fig. 7b). Values were slightly higher in autumn and winter (respectively 13.1±0.2 % and
310 11±2.1 % in cups #11 and #12) than in the summer, with the exception of cup #5 where the
311 highest value of 17.4 % was observed. PON fluxes followed the same seasonal patterns as
312 POC. This resulted in a relatively stable POC:PON ratio that varied between 6.1 to 7.4, except
313 in the autumn cup #11 where it exceeded 8.1 (Table 1).

314 **4 Discussion**

315 **4.1 Physical conditions of trap deployment**

316 Moored sediment traps can be subject to hydrodynamic biases that affect the accuracy of
317 particle collection (Buesseler et al., 2007a). The aspect ratio, tilt and horizontal flow regimes
318 are important considerations when assessing sediment trap performance. Specifically, the line
319 angle and aspect ratio of cylindrical traps can result in oversampling (Hawley, 1988).
320 Horizontal current velocities of 12 cm s⁻¹ are often invoked as a critical threshold over which
321 particles are no longer quantitatively sampled (Baker et al., 1988). During the sediment trap

322 deployment period we observed generally low current speeds (mean $< 10 \text{ cm s}^{-1}$) with 75% of
323 the recorded data lower than 12 cm s^{-1} . Despite the high aspect ratio of the PPS3 trap (4.75),
324 and the small mooring line angle deviations, it is likely that episodic increases in current
325 velocities ($>12 \text{ cm s}^{-1}$) impacted collection efficiency. When integrated over the entire current
326 meter record (October 2011 to April 2012), the resulting flow is consistent with the annual
327 northeastward, low velocity ($\sim 1 \text{ cm s}^{-1}$) geostrophic flow previously reported over the
328 central part of the Kerguelen plateau (Park et al., 2008b).

329 The depth of the winter mixed layer (WML) on the Kerguelen Plateau is usually
330 shallower than 250 m (Park et al., 1998; Metzl et al., 2006). The sediment trap deployment
331 depth of $\sim 300 \text{ m}$ was selected to sample particle flux exiting the WML. The moored CTD
332 sensor did not record any evidence of a winter water incursion during the deployment period,
333 confirming the WML did not reach the trap depth. The small depth variations observed during
334 the deployment period resulted from vertical displacement of the trap. Variations of σ_θ may
335 have resulted from both vertical displacement of the CTD sensor and possible isopycnal
336 displacements due to strong internal waves that can occur with an amplitude of $> 50 \text{ m}$ at this
337 depth (Park et al., 2008a). Our measurements demonstrate that isopycnal displacements are
338 consistent with the M2 (moon 2, 12.4 h period) tidal forcing described in physical modeling
339 studies (Maraldi et al., 2009, 2011). Spectral analysis indicates that high frequency tidal
340 currents are the major circulation components. Time-integrated currents ~~shows~~ suggest that
341 advection is weak and occurs over longer timescale (months). Assuming the current flow
342 measured at the sediment trap deployment depth is representative of the prevailing current
343 under the WML, more than three months are required for particles to leave the plateau from
344 the A3 station, a timescale larger than the bloom duration itself. Therefore we consider that
345 the particles collected in the sediment trap at station A3 were produced in the surface waters
346 located above the plateau during bloom conditions.

347

4.2 Swimmers and particle solubilization

348 Aside from the hydrodynamic effects discussed above, other potential biases characterizing
349 sediment trap deployments, particularly those in shallow waters, is the presence of swimmers
350 and particle solubilization. Swimmers can artificially increase POC fluxes by entering the
351 cups and releasing particulate organic matter or decrease the flux by feeding in the trap funnel
352 (Buesseler et al., 2007a). ~~Swimmers were most abundant in the cups #8 to #12 (January to~~
353 ~~September 2012) generally through the representation of copepods and amphipods (Table 2).~~
354 ~~Some studies have focused specifically on swimmer communities collected in shallow~~
355 ~~sediment traps (Matsuno et al., 2014 and references therein) although trap collection of~~
356 ~~swimmers is probably selective and therefore not quantitative. Total swimmer intrusion rate~~
357 ~~was highest in cups #6 to #9 (December 2011 to February 2012) generally through the~~
358 ~~representation of copepods and amphipods (Table 2) The maximum swimmer intrusion rate in~~
359 ~~mid-summer as well as the copepod dominance is consistent with the fourfold increase in~~
360 ~~mesozooplankton abundance observed from winter to summer (Carlotti et al., 2014).~~
361 ~~However,~~ Swimmer abundance was not correlated with mass flux, POC or PON fluxes,
362 suggesting that their presence did not ~~notably systematically-~~ affected particulate fluxes inside
363 the cups. Nevertheless such correlations ~~are not diagnostic and we~~ cannot rule out the
364 possibility of swimmers feeding in the trap funnel modifying particle flux collection. ~~during~~
365 ~~this study.~~

366 Particle solubilization in preservative solutions ~~can lead~~ may also lead to an
367 underestimation of total flux measured in sediment traps. ~~Previous a~~Analyses from traps
368 poisoned with mercuric chloride suggest that ~30 % of total organic carbon flux can be found
369 in the dissolved phase and much higher values of 50 % and 90 % may be observed for
370 nitrogen and phosphorous, respectively (Antia, 2005; O'Neill et al., 2005). Unfortunately the
371 use of a formaldehyde-based preservative in our trap samples precludes any direct estimate of

372 excess of dissolved organic carbon in the sample cup supernatant. Furthermore, corrections
373 for particle leaching have been considered problematic in the presence of swimmers since a
374 fraction of the leaching may originate from the swimmers themselves (Antia, 2005),
375 potentially leading to over-correction. ~~This Particles solubilization may have occurred in our~~
376 ~~samples as evidenced by excess high PO₄³⁻ excess was found~~ in the supernatant. ~~of~~ However
377 ~~the largest values were measured in sample~~ cups where total swimmers were abundant (cups
378 #8 to #12, data not shown). ~~Therefore~~ Consequently, it was not ~~im~~possible to ~~discriminate~~
379 ~~solubilisation of P from swimmers and passively settling particles and it therefore remains~~
380 ~~difficult to quantify the effect of particle leaching. accurately correct export fluxes for particle~~
381 ~~leaching. However, considering the typical leaching values for POC of 30 % reported in the~~
382 ~~literature (Antia, 2005; O'Neill et al., 2005) it is unlikely that solubilization of organic matter~~
383 ~~from passively settling particles exerts a major impact on our flux determination.~~ However,
384 leaching of POC should be less problematic in formalin-preserved samples because aldehydes
385 fix organic matter, rather than ~~just~~ poisoning microbial activity.

386 ~~4.3. Rapid flux attenuation at A3~~

387 ~~4.3 Seasonal dynamic of POC export~~

388 ~~The sediment trap record obtained from station A3 provides the first direct estimate of POC~~
389 ~~export covering an entire season over the naturally fertilized Kerguelen Plateau. We observed~~
390 ~~a temporal lag of one month between the two surface chlorophyll *a* peaks and the two export~~
391 ~~events. Based on a compilation of annual sediment trap deployments Lutz et al. (2007)~~
392 ~~reported that export quickly follows primary production at low latitudes whereas a time lag up~~
393 ~~to two months could occur at higher latitudes. A 1-2 month lag was observed between~~
394 ~~production and export in the pacific sector of the Southern Ocean (Buesseler et al., 2001), as~~
395 ~~well as along 170°W (Honjo et al., 2000) and in the Australian sector of the Subantarctic~~

396 Zone (Rigual-Hernández et al., 2015). The temporal lag between surface production and
397 measured export in deep traps can originate from ecological processes in the upper ocean
398 (e.g. carbon retention in the mixed layer) as well as slow sinking velocities (Armstrong et al.,
399 2009) and one cannot differentiate the two processes from a single deep trap signal. A global-
400 scale modeling study suggests that the strongest temporal decoupling between production and
401 export (more than one month) occurs in areas characterized by a strong seasonal variability in
402 primary production (Henson et al., 2014). The study attributes this decoupling to differences
403 in phenology of phytoplankton and zooplankton and evokes zooplankton ejection products as
404 major contributors to fast sinking particles sedimenting post bloom.

405 On the Kerguelen Plateau there is evidence that a significant fraction of
406 phytoplankton biomass comprising the two chlorophyll peaks is remineralized by a highly
407 active heterotrophic microbial community (Obenosterer et al., 2008; Christaki et al., 2014).
408 Another fraction likely is channeled toward higher trophic levels through the intense grazing
409 pressure that support the observed increase in zooplankton biomass (Carlotti et al.,
410 2008,2014). Therefore an important fraction of phytoplankton biomass increases observed by
411 satellite may not contribute to export fluxes. Notably, the POC:PON ratio measured in our
412 trap material is close to values reported for marine diatoms (7.3 ± 1.2 , Sarthou et al., 2005),
413 compared to the C:N ratio of zooplankton faecal pellets which is typically higher (7.3 to >15,
414 Gerber and Gerber, 1979; Checkley and Entzeroth, 1985; Morales, 1987). Simple mass
415 balance would therefore suggest a significant contribution of phytoplanktonic cells to the
416 POC export, which is indeed corroborated by detailed microscopic analysis (Rembauville et
417 al., 2014).

418 Although we observed increasing contribution of faecal pellet carbon post-bloom
419 (Rembauville et al., 2014), in line with the model output of Henson et al. (2014), differences
420 in phytoplankton and zooplankton phenology do not fully explain the seasonality of export on

421 the Kerguelen Plateau. Considering the shallow trap depth (289 m) and typical sinking speed
422 of 100 m d^{-1} for phyto-aggregates (Allredge and Gotschalk, 1988; Peterson et al., 2005; Trull
423 et al., 2008a), aggregate-driven export following bloom demise would suggest a short lag of a
424 few days between production and export peaks. The temporal lag of one month measured in
425 the present study suggest either slow sinking rates ($<5 \text{ m d}^{-1}$) characteristic of single
426 phytoplanktonic cells or faster sinking particles that do not originate from the peaks of surface
427 production. It is generally accepted that satellite detection depth is 20-50 m (Gordon and
428 McCluney, 1975), which prevents the detection of deep phytoplanktonic biomass structures
429 (Villareal et al., 2011). Although subsurface chlorophyll maximum located around 100 m
430 have been observed over the Kerguelen Plateau at the end of the productive period, they have
431 been interpreted to result from the accumulation of surface production at the base of the
432 mixed layer rather than a subsurface productivity feature (Uitz et al., 2009). In support of this
433 detailed taxonomic analysis of the exported material highlight diatom resting spores as major
434 contributors to the two export fluxes rather than a composite surface community accumulated
435 at the base of the mixed layer. The hypothesis of a mass production of nutrient-limited resting
436 spores post-bloom with high settling rates explains the temporal patterns of export we
437 observed (Rembauville et al., 2014). However a better knowledge of the dynamics of factors
438 responsible for resting spore formation by diatoms remains necessary to fully validate this
439 hypothesis.

440

441 **4.4 Rapid flux attenuation over the Kerguelen Plateau**

442 ~~The annual POC export of $\sim 0.1 \text{ mol m}^{-2} \text{ d}^{-1}$ at $\sim 300 \text{ m}$ (Table 1) is significantly lower than~~
443 ~~indirect estimates of POC export ($5.1 \text{ mol m}^{-2} \text{ d}^{-1}$) at the base of the WML (200 m) on the~~
444 ~~Kerguelen Plateau (Blain et al., 2007).~~ The Kerguelen Plateau annual POC export (98.2 ± 4.4
445 $\text{mmol m}^{-2} \text{ y}^{-1}$) approaches the median global ocean POC export value comprising shallow and

446 deep sediment traps ($83 \text{ mmol m}^{-2} \text{ y}^{-1}$, Lampitt and Antia, 1997), but is also close to values
447 observed in HNLC areas of the POOZ ($11\text{-}43 \text{ mmol m}^{-2} \text{ y}^{-1}$ at 500 m, Fischer et al., 2000).
448 Moreover, the magnitude of annual POC export measured at $\sim 300\text{m}$ on the Kerguelen Plateau
449 is comparable to deep-ocean ($>2 \text{ km}$) POC fluxes measured from the iron-fertilized Crozet
450 ($60 \text{ mmol m}^{-2} \text{ y}^{-1}$, Salter et al., 2012) and South Georgia blooms ($180 \text{ mmol m}^{-2} \text{ y}^{-1}$, Manno et
451 al., 2014).

452 The annual POC export of $\sim 0.1 \text{ mol m}^{-2} \text{ y}^{-1}$ at 289 m (Table 1) represents only 2% of
453 the indirect estimate of POC export ($5.1 \text{ mol m}^{-2} \text{ y}^{-1}$) at the base of the WML (200 m) on the
454 Kerguelen Plateau based on a seasonal DIC budget (Blain et al., 2007). On shorter time
455 scales, the POC flux recorded in the moored sediment trap represents only a small fraction (3-
456 8%) of the POC flux at the base of the winter mixed layer (200 m) measured by different
457 methods during KEOPS2 (Table 3). The same conclusion is true when considering the
458 comparison with different estimates made during KEOPS1. The diversity of the methods and
459 the difference in the depth where the POC flux was estimated render quantitative comparisons
460 challenging, but it appears the POC fluxes measured at 289 m with the moored sediment trap
461 are considerably lower than some other estimates. This result indicates either extremely rapid
462 attenuation of flux between 200 m and 300 m or major sampling bias by the sediment trap.

463 We note that low carbon export fluxes around 300 m have been previously reported on
464 the Kerguelen plateau. In spring 2011, UVP derived estimates of POC export at 350 m equals
465 0.1 to $0.3 \text{ mmol m}^{-2} \text{ d}^{-1}$ (Table 3), a value close to our reported value of $0.15 \text{ mmol m}^{-2} \text{ d}^{-1}$. In
466 summer 2005, POC export at 330 m from gel trap equals $0.7 \text{ mmol m}^{-2} \text{ d}^{-1}$ (Ebersbach and
467 Trull 2008), which is also close to our value of $1.5 \text{ mmol m}^{-2} \text{ d}^{-1}$. Using the Jouandet et al.
468 (2014) data at 200 m ($1.9 \text{ mmol m}^{-2} \text{ d}^{-1}$) and 350 m ($0.3 \text{ mmol m}^{-2} \text{ d}^{-1}$) and the Ebersbach and
469 Trull (2008) data at 200 m ($5.2 \text{ mmol m}^{-2} \text{ d}^{-1}$) and 330 m ($0.7 \text{ mmol m}^{-2} \text{ d}^{-1}$) leads to Martin
470 power law exponents values of 3.3 and 4, respectively. These values are high when compared

471 to the range of 0.4–1.7 that was initially compiled for the global ocean (Buesseler et al.,
472 2007b). However, there is increasing evidence in support of much higher b-values in the
473 Southern Ocean that fall in the range 0.9-3.9 (Lam and Bishop, 2007; Henson et al., 2012;
474 Cavan et al., 2015). Our calculations are thus consistent with emerging observations in the
475 Southern Ocean and support a scenario of strong POC flux attenuation between 200 m and
476 350 m over the Kerguelen Plateau

477 Using the aforementioned b values (3.3 and 4) and the POC flux derived from ^{234}Th
478 deficit at 200 m in spring (Planchon et al., 2014), we estimate POC fluxes at 289 m of 0.7 to
479 $1.1 \text{ mmol m}^{-2} \text{ d}^{-1}$. The flux measured in our sediment trap ($0.15 \text{ mmol m}^{-2} \text{ d}^{-1}$) data represents
480 14 % to 21 % of this calculated flux. Very similar percentages (21 % to 27 %) are found using
481 the POC fluxes derived from the ^{234}Th deficit in summer (Savoye et al., 2008). Therefore we
482 consider that the moored sediment trap collected ~15-30 % of the particle flux throughout the
483 year. Trap-derived particle fluxes can represent 0.1 to >3 times the ^{234}Th -derived particles in
484 shallow sediment traps (Buesseler, 1991; Buesseler et al., 1994; Coppola et al., 2002;
485 Gustafsson et al., 2004) and this difference is largely attributed to the sum of hydrodynamic
486 biases and swimmer activities (Buesseler, 1991), although it probably also includes the effect
487 of post-collection particle solubilisation. In the Antarctic Peninsula, ^{234}Th derived POC export
488 was 20 times higher than the fluxes collected by a shallow, cylindrical, moored sediment trap
489 at 170 m (Buesseler et al., 2010). The present deployment context is less extreme (depth of
490 289 m, mean current speed $<10 \text{ cm s}^{-1}$, low tilt angle, high aspect ratio of the cylindrical PPS3
491 trap) but we consider that hydrodynamics (current speed higher than 12 cm s^{-1} during short
492 tidal-driven events) and possible zooplankton feeding on the trap funnel are potential biases
493 that may explain in part the low fluxes recorded by the moored sediment trap. Therefore the
494 low fluxes observed likely result from a combination of collection bias (hydrodynamics and
495 swimmers) and strong attenuation of the POC flux between the base of the WML and 300 m

496 Despite our conclusion that the moored sediment trap deployment was characterized
497 by a low collection efficiency of ~15-30% with reference to ²³⁴Th-derived fluxes, the
498 numerous lines of evidence discussed above appear to converge on a scenario of rapid flux
499 attenuation. Strong POC flux attenuation over the Kerguelen Plateau compared to the open
500 ocean is also reported by Laurenceau et al. (2014) who associate this characteristic to a HBLE
501 scenario and invoke the role of mesozooplankton in the carbon flux attenuation. Between
502 October and November 2011, mesozooplankton biomass in the mixed layer doubled (Carlotti
503 et al., 2014) and summer biomass was twofold higher still (Carlotti et al., 2008). These
504 seasonal patterns are consistent with the maximum swimmer intrusion rate and swimmer
505 diversity observed in summer (Table 2). It has previously been concluded that zooplankton
506 biomass is more tightly coupled to phytoplankton biomass on the plateau compared to oceanic
507 waters, leading to higher secondary production on the plateau (Carlotti et al., 2008, 2014).
508 Further support linking zooplankton dynamics to HBLE environments of iron-fertilized
509 blooms are the findings of Cavan et al. (2015) that documents lowest export ratio (exported
510 production/primary production) in the most productive, naturally fertilized area downstream
511 of South Georgia. Another important ecosystem feature associated to the HBLE environment
512 of the Kerguelen Plateau, and likely shared by other island-fertilized blooms in the Southern
513 Ocean, is the presence of mesopelagic fishes (myctophid spawning and larvae foraging site,
514 Koubbi et al., 1991, 2001). Mesopelagic fishes can be tightly coupled to lower trophic levels
515 (Saba and Steinberg, 2012) and can play a significant role in carbon flux attenuation (Davison
516 et al., 2013). Although important for carbon budgets it is a compartment often neglected due
517 to the challenge of quantitative sampling approaches. We suggest that the HBLE scenario and
518 large attenuation of carbon flux beneath the WML at Kerguelen may represents the transfer of
519 carbon biomass to higher and mobile trophic groups that fuel large mammal and bird
520 populations rather than the classical remineralization-controlled vertical attenuation

521 characterizing open ocean environments. Although technically challenging, testing this
522 hypothesis should be a focus for future studies in this and similar regions.

523 ~~The POC fluxes we measured at 300 m on the Kerguelen Plateau are low and raise~~
524 ~~some questions about possible bias in the sediment trap measurements. The current data do~~
525 ~~not seem to support a significant hydrodynamic effect in the collection of particles, but~~
526 ~~unfortunately we do not have independent radionuclide data to support this conclusion. Trap-~~
527 ~~derived particle fluxes can represent 0.1 to >3 times the ²³⁴Th derived particles in shallow~~
528 ~~sediment traps (Buesseler, 1991; Buesseler et al., 1994; Coppola et al., 2002; Gustafsson et~~
529 ~~al., 2004) and this difference is largely attributed to the sum of hydrodynamic biases and~~
530 ~~swimmer activities (Buesseler, 1991), although it probably also includes the effect of post-~~
531 ~~collection particle solubilisation. Even if we assume that our A3 sediment trap did~~
532 ~~undersample the particle flux, it seems unlikely that this in itself could explain the significant~~
533 ~~reduction in POC flux observed between 200 m and 300 m (Table 3). Although we are unable~~
534 ~~to completely eliminate the possibility of some bias in our sediment trap measurements, the~~
535 ~~coherence between our observations and independent techniques (Table 3) indicate that the~~
536 ~~rapid attenuation of flux beneath the WML is a genuine ecological feature of the Kerguelen~~
537 ~~Plateau bloom.~~

538 ~~To further investigate the possibility of rapid flux attenuation on the Kerguelen~~
539 ~~Plateau, the sediment trap flux data were compared with parallel estimates of POC export~~
540 ~~conducted during the KEOPS2 field campaign. POC export at A3 was measured in drifting~~
541 ~~sediment traps (Laurenceau et al., 2014b), derived from ²³⁴Th deficit (Planchon et al. 2014)~~
542 ~~and from particles abundances measured with an Underwater Video Profiler (UVP) (Jouandet~~
543 ~~et al., 2014). These measurements occurred during the two visits (A3-1; 20 to 21 October~~
544 ~~2011, and A3-2; 16 November 2011) and coincided with the opening of the cups #1 and #2 of~~
545 ~~the moored sediment trap (Fig. 8). Between the 21 October and the 16 November 2011, the~~

546 mean POC concentration in the mixed layer increased by almost a factor of three but
547 remained similar at 300 m with a mean value of 3.8 μM . During the same interval, POC
548 fluxes at 200 m derived from ^{234}Th (Planchon et al., 2014) did not change significantly.
549 However in November, the ^{234}Th -derived POC fluxes were in the same range as 200 m UVP
550 estimates ($1.9\text{--}3.8\text{ mmol m}^{-2}\text{d}^{-1}$) that exhibited a 13-fold increase between the two sampling
551 dates, a fact attributed to intense algal aggregation (Jouandet et al., 2014). The POC fluxes
552 measured in the moored sediment trap at 300 m and the UVP estimates at 350 m did not
553 change significantly during this time. The POC fluxes observed at >300 m by both techniques
554 were low ($<0.25\text{ mmol m}^{-2}\text{d}^{-1}$) compared to the 200 m fluxes. POC fluxes in the third
555 sampling cup (open until beginning of December) were also low ($0.15\text{ mmol m}^{-2}\text{d}^{-1}$; Table 1).

556 The daily POC export fluxes measured at A3 by the moored sediment trap were also
557 compared with 2005 summer cruise flux estimates measured during KEOPS1 (Table 3). The
558 diversity of approaches prevents absolute comparison of the fluxes, however there are several
559 notable trends. The measurement of these fluxes at the end of the 2005 bloom is concomitant
560 with the highest recorded POC fluxes measured by the A3 sediment trap during the 2011
561 bloom (Fig. 7b). Most of these previous estimates were made at depths <200 m and are one
562 to two orders of magnitude greater than the maximum observed A3 sediment trap flux (~ 300
563 m) of $1.6\text{ mmol m}^{-2}\text{d}^{-1}$ measured in December (Table 1). Similarly low estimates of 0.7 and 1
564 $\text{mmol m}^{-2}\text{d}^{-1}$ were measured during KEOPS1 in drifting gel traps at 330 m and 430 m,
565 respectively (Ebersbach and Trull, 2008). Therefore, rapid flux attenuation beneath the base
566 of the WML (200 m) appears to be a feature observed during both spring and summer periods.

567 To constrain the magnitude of flux attenuation, 200 m and 300 m POC fluxes during
568 spring and summer were compared using a power law curve (Martin et al., 1987). A classical
569 range for the b exponent (0.4 to 1.7) is equivalent to a reduction in POC flux between 200 and
570 300 m of $\sim 15\text{--}55\%$. Here we used the ^{234}Th fluxes (Planchon et al. 2014) and UVP estimates

571 (~~Jouandet et al., 2014~~) at 200 m in spring and ~~^{234}Th fluxes (Savoie et al., 2008)~~ and drifting
572 gel trap estimates (~~Ebersbach and Trull, 2008~~) at 200 m in summer, with the congruent POC
573 fluxes from the A3 moored sediment trap at 289 m. The calculation yields ~~b~~ values of 7–11.3,
574 which equates POC flux attenuation of 94–96 % over a 100 m depth interval. These estimates
575 from spring and summer are comparable with the 98 % reduction in POC flux from 5.1 mol
576 $\text{m}^{-2} \text{ yr}^{-1}$ at 200m (~~Blain et al., 2007~~) to $0.1 \text{ mol m}^{-2} \text{ yr}^{-1}$ (this study) inferred from the
577 comparison of annual flux budgets over the same depth interval. There is therefore consistent
578 evidence supporting rapid flux attenuation at the base of the WML over the Kerguelen Plateau
579 during the period of major annual bloom transfer to the sediments.

580 **4.4 Hypotheses for rapid flux attenuation**

581 The annual export of POC at 289 m is exceptionally low ($98.2 \pm 4.4 \text{ mmol m}^{-2} \text{ y}^{-1}$) compared to
582 estimates of seasonal net community carbon production ($6.6 \pm 2.2 \text{ mol m}^{-2}$; Jouandet et al.,
583 2008) and estimates of POC export at the base of the WML (5.1 mol m^{-2} ; Blain et al., 2007).
584 Retention and degradation of particulate material above the WML (220 m) may partially
585 explain the strong flux attenuation within and below the WML. The POC:PON ratio measured
586 in the trap material is close to the Redfield value for phytoplankton of 6.6 (Redfield, 1934) in
587 spring and summer, implying a significant contribution of phytoplanktonic cells to the
588 exported material, which is corroborated by detailed microscopic analysis (Rembauville et al.
589 2014). Sinking speed can vary from 1 m d^{-1} for single phytoplankton cells to $\sim 100 \text{ m d}^{-1}$ for
590 phytoaggregates (Allredge and Gotschalk, 1988; Peterson et al., 2005; Trull et al., 2008) and
591 can reach values $> 2000 \text{ m d}^{-1}$ for large fecal pellets (Turner, 2002). Given the shallow trap
592 depth (289 m), export via phytoaggregates following bloom demise would suggest a short lag
593 of a few days between the bloom peak (Fig. 7) and flux peaks (Turner, 2002; Honda et al.,
594 2006; Trull et al., 2008); Laurenceau et al., in press). However, the temporal lag measured in
595 our study is approximately one month, implying either slow settling rates characteristic of

596 ~~single cells or faster settling fluxes that do not originate from the peak in surface production.~~
597 ~~Slow sinking rates between surface production and export and may be a causal factor for the~~
598 ~~strong attenuation by allowing particles to be remineralized in the mixed layer and/or~~
599 ~~intercepted by higher trophic levels.~~

600 ~~The remineralization of particles by heterotrophic microbes is unlikely to completely~~
601 ~~account for this reduction in POC flux. In summer, the bacterial carbon production (BP) at~~
602 ~~200 m at station A3 is approximately $10 \text{ nmol L}^{-1} \text{ d}^{-1}$ and bacterial growth efficiency (BGE)~~
603 ~~range between 8–15 % (Obernosterer et al., 2008). Calculating the bacterial carbon demand~~
604 ~~(BCD = BP/BGE) and integrating it between 200 and 289 m suggests that a POC flux~~
605 ~~attenuation in the range of 5.9 to $11.1 \text{ mmol m}^{-2} \text{ d}^{-1}$ could be reasonably attributed to~~
606 ~~heterotrophic microbial activity. Although significant, this estimate cannot account for the~~
607 ~~difference between the POC flux at 200 m and 289 m (e.g. $22.9 \text{ mmol m}^{-2} \text{ d}^{-1}$ attenuation from~~
608 ~~$24.5 \text{ mmol m}^{-2} \text{ d}^{-1}$ to $1.6 \text{ mmol m}^{-2} \text{ d}^{-1}$ in summer; Table 3). Furthermore, these values are~~
609 ~~likely to be an overestimate because they imply bacterial production is exclusively controlled~~
610 ~~by particulate organic carbon and ignore the important role of dissolved carbon substrates.~~
611 ~~The Barium excess (Ba_{xs}) proxy provides an alternative estimate of carbon remineralization~~
612 ~~(Dehairs et al., 1997). Carbon remineralization rates integrated over 150–400 m are equal to~~
613 ~~0.9 – $1.2 \text{ mmol m}^{-2} \text{ d}^{-1}$ in spring (Jacquet et al., 2014) and 2.1 – $2.8 \text{ mmol m}^{-2} \text{ d}^{-1}$ in summer~~
614 ~~(Jacquet et al., 2008). These remineralisation rates are also too low to explain the observed~~
615 ~~attenuation in POC flux at the base of the mixed layer.~~

616 ~~Mesozooplankton biomass and community structure is reported for the A3 station in~~
617 ~~spring and summer in Carlotti et al., (2014) and Carlotti et al., (2008), respectively. Between~~
618 ~~October and November 2011, mesozooplankton biomass in the mixed layer doubled (Carlotti~~
619 ~~et al., 2014). In summer (January 2005), the observed mesozooplankton biomass was again~~
620 ~~twofold higher than in spring 2011 (Carlotti et al., 2008). It was concluded that the~~

621 zooplankton community structure was able to answer more rapidly to phytoplankton biomass
622 availability on the plateau compared to oceanic water, leading to higher secondary production
623 on the plateau (Carlotti et al., 2008, 2014). Efficient grazers such as *Oithona similis* (McLeod
624 et al., 2010; Pinkerton et al., 2010), that also exhibit coprophagy, may increase carbon
625 retention in higher trophic compartments (Gonzalez and Smetacek, 1994). Furthermore, it is
626 possible that vertical migrating zooplankton communities produce fecal pellets below the trap
627 deployment depth. Notably, *Oithona similis* represents > 50 % of the mesozooplankton
628 assemblage at the station A3 in spring (Carlotti et al., 2014) whereas the summer community
629 structure is more diversified, containing small copepods but also larger calanoid copepods,
630 pteropods and amphipods (Carlotti et al., 2008). This is consistent with the maximum
631 swimmer intrusion rate and swimmer diversity observed in summer (Table 2). A study in the
632 North Pacific supports the significance of mesopelagic fish communities for carbon flux
633 attenuation (Davison et al., 2013). Although important for carbon budgets it is a compartment
634 often neglected due to the challenge of quantitative sampling approaches. Mesopelagic fish
635 larvae are known to be abundant on the southern part of the Kerguelen plateau (myctophid
636 spawning and larvae foraging site, Koubbi et al., 1991, 2001). We offer the hypothesis that a
637 significant fraction of net community production is channeled to higher trophic levels through
638 mesozooplankton dynamics and possibly myctophid fishes that fuel large mammal and bird
639 populations around the productive iron fertilized Kerguelen Plateau. Therefore high grazing
640 pressure and an efficient shift of carbon biomass to predatory mammals and birds may be
641 responsible for the HBLE scenario encountered on the productive iron fertilized Kerguelen
642 Plateau.

643

644 5. Conclusion

645 We have reported the seasonal dynamics of particulate organic carbon (POC) export under the
646 winter mixed layer (289 m) of the naturally fertilized, productive central Kerguelen Plateau.
647 Annual POC flux was very low (98 mmol m^{-2}) and most of it occurred during two episodic
648 (<14 days) events exported with a 1 month lag following two surface chlorophyll *a* peaks.
649 ~~Analysis of the hydrological conditions didn't support strong hydrodynamic biases that could~~
650 ~~explain the low fluxes observed. A comparison with different estimates of POC fluxes in~~
651 ~~spring and summer at the same station allowed to identify a strong flux attenuation between~~
652 ~~the basis of the mixed layer and the sediment trap depth. Bacterial heterotrophic activity in the~~
653 ~~upper mesopelagic is not enough to explain the observed attenuation.~~ Analysis of the
654 hydrological conditions and a comparison with different estimates of POC fluxes in spring
655 and summer at the same station suggest that the sediment trap was subject to possible
656 hydrodynamic and biological biases leading to under collection of particle flux. Nevertheless
657 the low POC export was close to other estimates of deep (>300 m) POC export at the same
658 station ~~and is consistent with high attenuation coefficients reported from other methods.~~
659 ~~Taken together these data suggesting that the low fluxes were partly due to~~ can be explained
660 ~~in part by~~ strong flux attenuation between the winter mixed layer depth (~200 m) and the trap
661 depth (~300 m). ~~We invoke mesozooplankton and the activity of mesopelagic fishes as~~
662 ~~possible explanations for efficient carbon retention and/or transfer to higher trophic levels at~~
663 ~~the base of the mixed layer which results in a High Biomass, Low Export environment. We~~
664 ~~invoke mesozooplankton and possibly mesopelagic fishes activity for being responsible for~~
665 ~~efficient the carbon retention and/or transfer to higher trophic levels at the basis of the mixed~~
666 ~~layer as a possible explanation for the HBLE scenario observed.~~

667 The biogenic silicon, diatoms ~~assemblages~~ and faecal pellet fluxes are reported in a
668 companion paper that ~~aims to identify~~ identifies the primary ecological vectors ~~regulating the~~

669 magnitude of POC export and seasonal patterns in BSi:POC export ratios—~~that explain the~~
670 ~~intensity and the BSi:POC ratio of the fluxes~~ (Rembauville et al., 2014).

671 **Acknowledgements**

672 We thank the Chief Scientist Prof. Bernard Quéguiner, the Captain Bernard Lassiette and his
673 crew during the KEOPS2 mission on the R/V Marion Dufresne II. We thank Leanne Armand
674 and Tom Trull for their constructive comments, ~~as well as three anonymous reviewers~~ which
675 helped us to improve the manuscript. This work was supported by the French Research
676 program of INSU-CNRS LEFE-CYBER (Les enveloppes fluides et l'environnement – Cycles
677 biogéochimiques, environnement et ressources), the French ANR (Agence Nationale de la
678 Recherche, SIMI-6 program, ANR-10-BLAN-0614), the French CNES (Centre National
679 d'Etudes Spatiales) and the French Polar Institute IPEV (Institut Polaire Paul-Emile Victor).

- 681 Allredge, A.L., Gotschalk, C., 1988. In situ settling behavior of marine snow. *Limnol. Oceanogr.* 33, 339–351.
- 682 Aminot, A., Kerouel, R., 2007. Dosage automatique des nutriments dans les eaux marines: méthodes en flux
683 continu. Ifremer, Plouzané, France.
- 684 Antia, A.N., 2005. Solubilization of particles in sediment traps: revising the stoichiometry of mixed layer export.
685 *Biogeosciences* 2, 189–204. doi:10.5194/bg-2-189-2005
- 686 Armstrong, R.A., Peterson, M.L., Lee, C., Wakeham, S.G., 2009. Settling velocity spectra and the ballast ratio
687 hypothesis. *Deep Sea Res. Part II Top. Stud. Oceanogr.* 56, 1470–1478. doi:10.1016/j.dsr2.2008.11.032
- 688 Arrigo, K.R., Worthen, D., Schnell, A., Lizotte, M.P., 1998. Primary production in Southern Ocean waters. *J.*
689 *Geophys. Res. Oceans* 103, 15587–15600. doi:10.1029/98JC00930
- 690 Baker, E.T., Milburn, H.B., Tennant, D.A., 1988. Field assessment of sediment trap efficiency under varying
691 flow conditions. *J. Mar. Res.* 46, 573–592. doi:10.1357/002224088785113522
- 692 Barbeau, K., Moffett, J.W., Caron, D.A., Croot, P.L., Erdner, D.L., 1996. Role of protozoan grazing in relieving
693 iron limitation of phytoplankton. *Nature* 380, 61–64. doi:10.1038/380061a0
- 694 Batten, S.D., Gower, J.F.R., 2014. Did the iron fertilization near Haida Gwaii in 2012 affect the pelagic lower
695 trophic level ecosystem? *J. Plankton Res.* 36, 925–932. doi:10.1093/plankt/fbu049
- 696 Blain, S., Quéguiner, B., Armand, L., Belviso, S., Bombled, B., Bopp, L., Bowie, A., Brunet, C., Brussaard, C.,
697 Carloti, F., Christaki, U., Corbière, A., Durand, I., Ebersbach, F., Fuda, J.-L., Garcia, N., Gerringa, L.,
698 Griffiths, B., Guigue, C., Guillermin, C., Jaquet, S., Jeandel, C., Laan, P., Lefèvre, D., Lo Monaco, C.,
699 Malits, A., Mosseri, J., Obernosterer, I., Park, Y.-H., Picheral, M., Pondaven, P., Remenyi, T.,
700 Sandroni, V., Sarthou, G., Savoye, N., Scouarnec, L., Souhaut, M., Thuiller, D., Timmermans, K.,
701 Trull, T., Uitz, J., van Beek, P., Veldhuis, M., Vincent, D., Viollier, E., Vong, L., Wagener, T., 2007.
702 Effect of natural iron fertilization on carbon sequestration in the Southern Ocean. *Nature* 446, 1070–
703 1074. doi:10.1038/nature05700
- 704 Blain, S., Tréguer, P., Belviso, S., Bucciarelli, E., Denis, M., Desabre, S., Fiala, M., Martin Jézéquel, V., Le
705 Fèvre, J., Mayzaud, P., Marty, J.-C., Razouls, S., 2001. A biogeochemical study of the island mass
706 effect in the context of the iron hypothesis: Kerguelen Islands, Southern Ocean. *Deep Sea Res. Part*
707 *Oceanogr. Res. Pap.* 48, 163–187. doi:10.1016/S0967-0637(00)00047-9
- 708 Boltovskoy, D., 1999. South Atlantic zooplankton. *Backhuys*.
- 709 Bopp, L., Kohfeld, K.E., Le Quééré, C., Aumont, O., 2003. Dust impact on marine biota and atmospheric CO₂
710 during glacial periods. *Paleoceanography* 18, 1046. doi:10.1029/2002PA000810
- 711 Boyd, P.W., Jickells, T., Law, C.S., Blain, S., Boyle, E.A., Buesseler, K.O., Coale, K.H., Cullen, J.J., Baar,
712 H.J.W. de, Follows, M., Harvey, M., Lancelot, C., Levasseur, M., Owens, N.P.J., Pollard, R., Rivkin,
713 R.B., Sarmiento, J., Schoemann, V., Smetacek, V., Takeda, S., Tsuda, A., Turner, S., Watson, A.J.,
714 2007. Mesoscale Iron Enrichment Experiments 1993-2005: Synthesis and Future Directions. *Science*
715 315, 612–617. doi:10.1126/science.1131669
- 716 Boyd, P.W., Law, C.S., Hutchins, D.A., Abraham, E.R., Croot, P.L., Ellwood, M., Frew, R.D., Hadfield, M.,
717 Hall, J., Handy, S., Hare, C., Higgins, J., Hill, P., Hunter, K.A., LeBlanc, K., Maldonado, M.T., McKay,
718 R.M., Mioni, C., Oliver, M., Pickmere, S., Pinkerton, M., Safi, K., Sander, S., Sanudo-Wilhelmy, S.A.,
719 Smith, M., Strzepek, R., Tovar-Sanchez, A., Wilhelm, S.W., 2005. FeCycle: Attempting an iron
720 biogeochemical budget from a mesoscale SF6 tracer experiment in unperturbed low iron waters. *Glob.*
721 *Biogeochem. Cycles* 19, GB4S20. doi:10.1029/2005GB002494
- 722 Boyd, P.W., Trull, T.W., 2007. Understanding the export of biogenic particles in oceanic waters: Is there
723 consensus? *Prog. Oceanogr.* 72, 276–312. doi:10.1016/j.pocean.2006.10.007
- 724 Buesseler, K.O., 1991. Do upper-ocean sediment traps provide an accurate record of particle flux? *Nature* 353,
725 420–423. doi:10.1038/353420a0
- 726 Buesseler, K.O., Antia, A.N., Chen, M., Fowler, S.W., Gardner, W.D., Gustafsson, Ö., Harada, K., Michaels,
727 A.F., Rutgers v. d. Loeff, M., Sarin, M., Steinberg, D.K., Trull, T., 2007a. An assessment of the use of
728 sediment traps for estimating upper ocean particle fluxes. *J. Mar. Res.* 65, 345–416.
- 729 Buesseler, K.O., Ball, L., Andrews, J., Cochran, J.K., Hirschberg, D.J., Bacon, M.P., Flear, A., Brzezinski, M.,
730 2001. Upper ocean export of particulate organic carbon and biogenic silica in the Southern Ocean along
731 170°W. *Deep Sea Res. Part II Top. Stud. Oceanogr.* 48, 4275–4297. doi:10.1016/S0967-
732 0645(01)00089-3
- 733 Buesseler, K.O., Benitez-Nelson, C.R., Moran, S.B., Burd, A., Charette, M., Cochran, J.K., Coppola, L., Fisher,
734 N.S., Fowler, S.W., Gardner, W.D., Guo, L.D., Gustafsson, Ö., Lamborg, C., Masque, P., Miquel, J.C.,
735 Passow, U., Santschi, P.H., Savoye, N., Stewart, G., Trull, T., 2006. An assessment of particulate
736 organic carbon to thorium-234 ratios in the ocean and their impact on the application of ²³⁴Th as a
737 POC flux proxy. *Mar. Chem., Future Applications of ²³⁴Th in Aquatic Ecosystems (FATE)* 100, 213–
738 233. doi:10.1016/j.marchem.2005.10.013

739 Buesseler, K.O., Boyd, P.W., 2009. Shedding light on processes that control particle export and flux attenuation
740 in the twilight zone of the open ocean. *Limnol. Oceanogr.* 54, 1210–1232.
741 doi:10.4319/lo.2009.54.4.1210

742 Buesseler, K.O., Lamborg, C.H., Boyd, P.W., Lam, P.J., Trull, T.W., Bidigare, R.R., Bishop, J.K.B., Casciotti,
743 K.L., Dehairs, F., Elskens, M., Honda, M., Karl, D.M., Siegel, D.A., Silver, M.W., Steinberg, D.K.,
744 Valdes, J., Mooy, B.V., Wilson, S., 2007b. Revisiting Carbon Flux Through the Ocean's Twilight Zone.
745 *Science* 316, 567–570. doi:10.1126/science.1137959

746 Buesseler, K.O., McDonnell, A.M.P., Schofield, O.M.E., Steinberg, D.K., Ducklow, H.W., 2010. High particle
747 export over the continental shelf of the west Antarctic Peninsula. *Geophys. Res. Lett.* 37, L22606.
748 doi:10.1029/2010GL045448

749 Buesseler, K.O., Michaels, A.F., Siegel, D.A., Knap, A.H., 1994. A three dimensional time-dependent approach
750 to calibrating sediment trap fluxes. *Glob. Biogeochem. Cycles* 8, 179–193. doi:10.1029/94GB00207

751 Carlotti, F., Thibault-Botha, D., Nowaczyk, A., Lefèvre, D., 2008. Zooplankton community structure, biomass
752 and role in carbon fluxes during the second half of a phytoplankton bloom in the eastern sector of the
753 Kerguelen Shelf (January–February 2005). *Deep Sea Res. Part II Top. Stud. Oceanogr.* 55, 720–733.
754 doi:10.1016/j.dsr2.2007.12.010

755 Cavan, E.L., Le Moigne, F. a. c., Poulton, A.J., Tarling, G.A., Ward, P., Daniels, C.J., Fragoso, G., Sanders, R.J.,
756 2015. Zooplankton fecal pellets control the attenuation of particulate organic carbon flux in the Scotia
757 Sea, Southern Ocean. *Geophys. Res. Lett.* 2014GL062744. doi:10.1002/2014GL062744

758 Checkley, D.M., Entzeroth, L.C., 1985. Elemental and isotopic fractionation of carbon and nitrogen by marine,
759 planktonic copepods and implications to the marine nitrogen cycle. *J. Plankton Res.* 7, 553–568.
760 doi:10.1093/plankt/7.4.553

761 Christaki, U., Lefèvre, D., Georges, C., Colombet, J., Catala, P., Courties, C., Sime-Ngando, T., Blain, S.,
762 Obernosterer, I., 2014. Microbial food web dynamics during spring phytoplankton blooms in the
763 naturally iron-fertilized Kerguelen area (Southern Ocean). *Biogeosciences* 11, 6739–6753.
764 doi:10.5194/bg-11-6739-2014

765 Coale, K.H., Bruland, K.W., 1985. ^{234}Th : ^{238}U Disequilibria Within the California Current. *Limnol. Oceanogr.*
766 30, 22–33.

767 Coale, K.H., Johnson, K.S., Chavez, F.P., Buesseler, K.O., Barber, R.T., Brzezinski, M.A., Cochlan, W.P.,
768 Millero, F.J., Falkowski, P.G., Bauer, J.E., Wanninkhof, R.H., Kudela, R.M., Altabet, M.A., Hales,
769 B.E., Takahashi, T., Landry, M.R., Bidigare, R.R., Wang, X., Chase, Z., Strutton, P.G., Friederich,
770 G.E., Gorbunov, M.Y., Lance, V.P., Hilting, A.K., Hiscock, M.R., Demarest, M., Hiscock, W.T.,
771 Sullivan, K.F., Tanner, S.J., Gordon, R.M., Hunter, C.N., Elrod, V.A., Fitzwater, S.E., Jones, J.L.,
772 Tozzi, S., Koblizek, M., Roberts, A.E., Herndon, J., Brewster, J., Ladizinsky, N., Smith, G., Cooper, D.,
773 Timothy, D., Brown, S.L., Selph, K.E., Sheridan, C.C., Twining, B.S., Johnson, Z.I., 2004a. Southern
774 Ocean Iron Enrichment Experiment: Carbon Cycling in High- and Low-Si Waters. *Science* 304, 408–
775 414. doi:10.1126/science.1089778

776 Coale, K.H., Johnson, K.S., Chavez, F.P., Buesseler, K.O., Barber, R.T., Brzezinski, M.A., Cochlan, W.P.,
777 Millero, F.J., Falkowski, P.G., Bauer, J.E., Wanninkhof, R.H., Kudela, R.M., Altabet, M.A., Hales,
778 B.E., Takahashi, T., Landry, M.R., Bidigare, R.R., Wang, X., Chase, Z., Strutton, P.G., Friederich,
779 G.E., Gorbunov, M.Y., Lance, V.P., Hilting, A.K., Hiscock, M.R., Demarest, M., Hiscock, W.T.,
780 Sullivan, K.F., Tanner, S.J., Gordon, R.M., Hunter, C.N., Elrod, V.A., Fitzwater, S.E., Jones, J.L.,
781 Tozzi, S., Koblizek, M., Roberts, A.E., Herndon, J., Brewster, J., Ladizinsky, N., Smith, G., Cooper, D.,
782 Timothy, D., Brown, S.L., Selph, K.E., Sheridan, C.C., Twining, B.S., Johnson, Z.I., 2004b. Southern
783 Ocean Iron Enrichment Experiment: Carbon Cycling in High- and Low-Si Waters. *Science* 304, 408–
784 414. doi:10.1126/science.1089778

785 Coppola, L., Roy-Barman, M., Wassmann, P., Mulrow, S., Jeandel, C., 2002. Calibration of sediment traps and
786 particulate organic carbon export using ^{234}Th in the Barents Sea. *Mar. Chem.* 80, 11–26.
787 doi:10.1016/S0304-4203(02)00071-3

788 Davison, P.C., Checkley Jr., D.M., Koslow, J.A., Barlow, J., 2013. Carbon export mediated by mesopelagic
789 fishes in the northeast Pacific Ocean. *Prog. Oceanogr.* 116, 14–30. doi:10.1016/j.pocean.2013.05.013

790 De Baar, H.J.W., Boyd, P.W., Coale, K.H., Landry, M.R., Tsuda, A., Assmy, P., Bakker, D.C.E., Bozec, Y.,
791 Barber, R.T., Brzezinski, M.A., Buesseler, K.O., Boyé, M., Croot, P.L., Gervais, F., Gorbunov, M.Y.,
792 Harrison, P.J., Hiscock, W.T., Laan, P., Lancelot, C., Law, C.S., Levasseur, M., Marchetti, A., Millero,
793 F.J., Nishioka, J., Nojiri, Y., van Oijen, T., Riebesell, U., Rijkenberg, M.J.A., Saito, H., Takeda, S.,
794 Timmermans, K.R., Veldhuis, M.J.W., Waite, A.M., Wong, C.-S., 2005. Synthesis of iron fertilization
795 experiments: From the Iron Age in the Age of Enlightenment. *J. Geophys. Res. Oceans* 110, C09S16.
796 doi:10.1029/2004JC002601

797 De Baar, H.J.W., Buma, A.G.J., Nolting, R.F., Cadée, G.C., Jacques, G., Tréguer, P., 1990. On iron limitation of
798 the Southern Ocean: experimental observations in the Weddell and Scotia Seas. *Mar. Ecol. Prog. Ser.*
799 65, 105–122. doi:doi:10.3354/meps065105

800 Dehairs, F., Shopova, D., Ober, S., Veth, C., Goeyens, L., 1997. Particulate barium stocks and oxygen
801 consumption in the Southern Ocean mesopelagic water column during spring and early summer:
802 relationship with export production. *Deep Sea Res. Part II Top. Stud. Oceanogr.* 44, 497–516.
803 doi:10.1016/S0967-0645(96)00072-0

804 Dilling, L., Alldredge, A.L., 2000. Fragmentation of marine snow by swimming macrozooplankton: A new
805 process impacting carbon cycling in the sea. *Deep Sea Res. Part Oceanogr. Res. Pap.* 47, 1227–1245.
806 doi:10.1016/S0967-0637(99)00105-3

807 Dunne, J.P., Sarmiento, J.L., Gnanadesikan, A., 2007. A synthesis of global particle export from the surface
808 ocean and cycling through the ocean interior and on the seafloor. *Glob. Biogeochem. Cycles* 21,
809 GB4006. doi:10.1029/2006GB002907

810 Ebersbach, F., Trull, T.W., 2008. Sinking particle properties from polyacrylamide gels during the Kerguelen
811 Ocean and Plateau compared Study (KEOPS): Zooplankton control of carbon export in an area of
812 persistent natural iron inputs in the Southern Ocean. *Limnol. Oceanogr.* 53, 212–224.
813 doi:10.4319/lo.2008.53.1.0212

814 Ebersbach, F., Trull, T.W., Davies, D.M., Bray, S.G., 2011. Controls on mesopelagic particle fluxes in the Sub-
815 Antarctic and Polar Frontal Zones in the Southern Ocean south of Australia in summer—Perspectives
816 from free-drifting sediment traps. *Deep Sea Res. Part II Top. Stud. Oceanogr.* 58, 2260–2276.
817 doi:10.1016/j.dsr2.2011.05.025

818 Fischer, G., Ratmeyer, V., Wefer, G., 2000. Organic carbon fluxes in the Atlantic and the Southern Ocean:
819 relationship to primary production compiled from satellite radiometer data. *Deep Sea Res. Part II Top.*
820 *Stud. Oceanogr.* 47, 1961–1997. doi:10.1016/S0967-0645(00)00013-8

821 Francois, R., Honjo, S., Krishfield, R., Manganini, S., 2002. Factors controlling the flux of organic carbon to the
822 bathypelagic zone of the ocean. *Glob. Biogeochem. Cycles* 16, 1087. doi:10.1029/2001GB001722

823 Gall, M.P., Strzepak, R., Maldonado, M., Boyd, P.W., 2001. Phytoplankton processes. Part 2: Rates of primary
824 production and factors controlling algal growth during the Southern Ocean Iron RElease Experiment
825 (SOIREE). *Deep Sea Res. Part II Top. Stud. Oceanogr.*, The Southern Ocean Iron Release Experiment
826 (SOIREE) 48, 2571–2590. doi:10.1016/S0967-0645(01)00009-1

827 Gehlen, M., Bopp, L., Emprin, N., Aumont, O., Heinze, C., Ragueneau, O., 2006. Reconciling surface ocean
828 productivity, export fluxes and sediment composition in a global biogeochemical ocean model.
829 *Biogeosciences* 3, 521–537. doi:10.5194/bg-3-521-2006

830 Gerber, R.P., Gerber, M.B., 1979. Ingestion of natural particulate organic matter and subsequent assimilation,
831 respiration and growth by tropical lagoon zooplankton. *Mar. Biol.* 52, 33–43. doi:10.1007/BF00386855

832 Giering, S.L.C., Sanders, R., Lampitt, R.S., Anderson, T.R., Tamburini, C., Boutrif, M., Zubkov, M.V., Marsay,
833 C.M., Henson, S.A., Saw, K., Cook, K., Mayor, D.J., 2014. Reconciliation of the carbon budget in the
834 ocean's twilight zone. *Nature* 507, 480–483. doi:10.1038/nature13123

835 Gilman, D.L., Fuglister, F.J., Mitchell, J.M., 1963. On the Power Spectrum of “Red Noise.” *J. Atmospheric Sci.*
836 20, 182–184. doi:10.1175/1520-0469(1963)020<0182:OTPSON>2.0.CO;2

837 Gonzalez, H.E., Smetacek, V., 1994. The possible role of the cyclopoid copepod *Oithona* in retarding vertical
838 flux of zooplankton faecal material. *Mar. Ecol.-Prog. Ser.* 113, 233–246.

839 Gordon, H.R., McCluney, W.R., 1975. Estimation of the depth of sunlight penetration in the sea for remote
840 sensing. *Appl. Opt.* 14, 413–416.

841 Gruber, N., Gloor, M., Mikaloff Fletcher, S.E., Doney, S.C., Dutkiewicz, S., Follows, M.J., Gerber, M.,
842 Jacobson, A.R., Joos, F., Lindsay, K., Menemenlis, D., Mouchet, A., Müller, S.A., Sarmiento, J.L.,
843 Takahashi, T., 2009. Oceanic sources, sinks, and transport of atmospheric CO₂. *Glob. Biogeochem.*
844 *Cycles* 23, GB1005. doi:10.1029/2008GB003349

845 Gustafsson, O., Andersson, P., Roos, P., Kukulska, Z., Broman, D., Larsson, U., Hajdu, S., Ingri, J., 2004.
846 Evaluation of the collection efficiency of upper ocean sub-photoc-layer sediment traps: A 24-month in
847 situ calibration in the open Baltic Sea using 234Th. *Limnol. Oceanogr. Methods* 2, 62–74.
848 doi:10.4319/lom.2004.2.62

849 Hawley, N., 1988. Flow in Cylindrical Sediment Traps. *J. Gt. Lakes Res.* 14, 76–88. doi:10.1016/S0380-
850 1330(88)71534-8

851 Henson, S.A., Sanders, R., Madsen, E., 2012. Global patterns in efficiency of particulate organic carbon export
852 and transfer to the deep ocean. *Glob. Biogeochem. Cycles* 26, GB1028. doi:10.1029/2011GB004099

853 Henson, S.A., Sanders, R., Madsen, E., Morris, P.J., Le Moigne, F., Quartly, G.D., 2011. A reduced estimate of
854 the strength of the ocean's biological carbon pump. *Geophys. Res. Lett.* 38, L04606.
855 doi:10.1029/2011GL046735

856 Henson, S.A., Yool, A., Sanders, R., 2014. Variability in efficiency of particulate organic carbon export: A
857 model study. *Glob. Biogeochem. Cycles* 29, GB4965. doi:10.1002/2014GB004965

858 Hiscock, W.T., Millero, F.J., 2005. Nutrient and carbon parameters during the Southern Ocean iron experiment
859 (SOFEX). *Deep Sea Res. Part Oceanogr. Res. Pap.* 52, 2086–2108. doi:10.1016/j.dsr.2005.06.010

860 Honda, M.C., Kawakami, H., Sasaoka, K., Watanabe, S., Dickey, T., 2006. Quick transport of primary produced
861 organic carbon to the ocean interior. *Geophys. Res. Lett.* 33, L16603. doi:10.1029/2006GL026466

862 Honjo, S., Francois, R., Manganini, S., Dymond, J., Collier, R., 2000. Particle fluxes to the interior of the
863 Southern Ocean in the Western Pacific sector along 170°W. *Deep Sea Res. Part II Top. Stud. Oceanogr.*
864 47, 3521–3548. doi:10.1016/S0967-0645(00)00077-1

865 Honjo, S., Manganini, S.J., Krishfield, R.A., Francois, R., 2008. Particulate organic carbon fluxes to the ocean
866 interior and factors controlling the biological pump: A synthesis of global sediment trap programs since
867 1983. *Prog. Oceanogr.* 76, 217–285. doi:10.1016/j.pocean.2007.11.003

868 Hudson, J.M., Steinberg, D.K., Sutton, T.T., Graves, J.E., Latour, R.J., 2014. Myctophid feeding ecology and
869 carbon transport along the northern Mid-Atlantic Ridge. *Deep Sea Res. Part Oceanogr. Res. Pap.* 93,
870 104–116. doi:10.1016/j.dsr.2014.07.002

871 Jacquet, S.H.M., Dehairs, F., Savoye, N., Obernosterer, I., Christaki, U., Monnin, C., Cardinal, D., 2008.
872 Mesopelagic organic carbon remineralization in the Kerguelen Plateau region tracked by biogenic
873 particulate Ba. *Deep Sea Res. Part II Top. Stud. Oceanogr.* 55, 868–879.
874 doi:10.1016/j.dsr.2007.12.038

875 JGOFS Sediment Trap Methods, 1994. , in: *Protocols for the Joint Global Ocean Flux Study (JGOFS) Core*
876 *Measurements. Intergovernmental Oceanographic Commission, Scientific Committee on Oceanic*
877 *Research Manual and Guides, UNESCO, pp. 157–164.*

878 Jouandet, M.P., Blain, S., Metzl, N., Brunet, C., Trull, T.W., Obernosterer, I., 2008. A seasonal carbon budget
879 for a naturally iron-fertilized bloom over the Kerguelen Plateau in the Southern Ocean. *Deep Sea Res.*
880 *Part II Top. Stud. Oceanogr., KEOPS: Kerguelen Ocean and Plateau compared Study* 55, 856–867.
881 doi:10.1016/j.dsr.2007.12.037

882 Jouandet, M.-P., Jackson, G.A., Carlotti, F., Picheral, M., Stemmann, L., Blain, S., 2014. Rapid formation of
883 large aggregates during the spring bloom of Kerguelen Island: observations and model comparisons.
884 *Biogeosciences* 11, 4393–4406. doi:10.5194/bg-11-4393-2014

885 Jouandet, M.-P., Trull, T.W., Guidi, L., Picheral, M., Ebersbach, F., Stemmann, L., Blain, S., 2011. Optical
886 imaging of mesopelagic particles indicates deep carbon flux beneath a natural iron-fertilized bloom in
887 the Southern Ocean. *Limnol. Oceanogr.* 56, 1130–1140. doi:10.4319/lo.2011.56.3.1130

888 Karleskind, P., Lévy, M., Memery, L., 2011. Subduction of carbon, nitrogen, and oxygen in the northeast
889 Atlantic. *J. Geophys. Res. Oceans* 116, C02025. doi:10.1029/2010JC006446

890 Kohfeld, K.E., Quéré, C.L., Harrison, S.P., Anderson, R.F., 2005. Role of Marine Biology in Glacial-Interglacial
891 CO₂ Cycles. *Science* 308, 74–78. doi:10.1126/science.1105375

892 Korb, R.E., Whitehouse, M., 2004. Contrasting primary production regimes around South Georgia, Southern
893 Ocean: large blooms versus high nutrient, low chlorophyll waters. *Deep Sea Res. Part Oceanogr. Res.*
894 *Pap.* 51, 721–738. doi:10.1016/j.dsr.2004.02.006

895 Koubbi, P., Duhamel, G., Hebert, C., 2001. Seasonal relative abundance of fish larvae inshore at Îles Kerguelen,
896 Southern Ocean. *Antarct. Sci.* 13, 385–392. doi:10.1017/S0954102001000542

897 Koubbi, P., Ibanez, F., Duhamel, G., 1991. Environmental influences on spatio-temporal oceanic distribution of
898 ichthyoplankton around the Kerguelen Islands (Southern Ocean). *Mar. Ecol. Prog. Ser.* 72, 225–238.

899 Lampitt, R.S., Antia, A.N., 1997. Particle flux in deep seas: regional characteristics and temporal variability.
900 *Deep Sea Res. Part Oceanogr. Res. Pap.* 44, 1377–1403. doi:10.1016/S0967-0637(97)00020-4

901 Lampitt, R.S., Boorman, B., Brown, L., Lucas, M., Salter, I., Sanders, R., Saw, K., Seeyave, S., Thomalla, S.J.,
902 Turnewitsch, R., 2008. Particle export from the euphotic zone: Estimates using a novel drifting
903 sediment trap, 234Th and new production. *Deep Sea Res. Part Oceanogr. Res. Pap.* 55, 1484–1502.
904 doi:10.1016/j.dsr.2008.07.002

905 Lam, P.J., Bishop, J.K.B., 2007. High biomass, low export regimes in the Southern Ocean. *Deep Sea Res. Part II*
906 *Top. Stud. Oceanogr.* 54, 601–638. doi:10.1016/j.dsr.2007.01.013

907 Lam, P.J., Doney, S.C., Bishop, J.K.B., 2011. The dynamic ocean biological pump: Insights from a global
908 compilation of particulate organic carbon, CaCO₃, and opal concentration profiles from the
909 mesopelagic. *Glob. Biogeochem. Cycles* 25, GB3009. doi:10.1029/2010GB003868

910 Landry, M.R., Constantinou, J., Latasa, M., Brown, S.L., Bidigare, R.R., Ondrusek, M.E., 2000. Biological
911 response to iron fertilization in the eastern equatorial Pacific (IronEx II). III. Dynamics of
912 phytoplankton growth and microzooplankton grazing. *Mar. Ecol. Prog. Ser.* 201, 57–72.
913 doi:10.3354/meps201057

914 Lasbleiz, M., Leblanc, K., Blain, S., Ras, J., Cornet-Barthaux, V., Hélias Nunige, S., Quéguiner, B., 2014.
915 Pigments, elemental composition (C, N, P, and Si), and stoichiometry of particulate matter in the

916 naturally iron fertilized region of Kerguelen in the Southern Ocean. *Biogeosciences* 11, 5931–5955.
917 doi:10.5194/bg-11-5931-2014

918 Laurenceau, E.C., Trull, T.W., Davies, D.M., Bray, S.G., Doran, J., Planchon, F., Carlotti, F., Jouandet, M.-P.,
919 Cavagna, A.-J., Waite, A.M., Blain, S., 2014. The relative importance of phytoplankton aggregates and
920 zooplankton fecal pellets to carbon export: insights from free-drifting sediment trap deployments in
921 naturally iron-fertilised waters near the Kerguelen plateau. *Biogeosciences Discuss* 11, 13623–13673.
922 doi:10.5194/bgd-11-13623-2014

923 Laws, E.A., D'Sa, E., Naik, P., 2011. Simple equations to estimate ratios of new or export production to total
924 production from satellite-derived estimates of sea surface temperature and primary production. *Limnol.*
925 *Oceanogr. Methods* 593–601. doi:10.4319/lom.2011.9.593

926 Laws, E.A., Falkowski, P.G., Smith, W.O., Ducklow, H., McCarthy, J.J., 2000. Temperature effects on export
927 production in the open ocean. *Glob. Biogeochem. Cycles* 14, 1231–1246. doi:10.1029/1999GB001229

928 Lefèvre, D., Guigue, C., Obernosterer, I., 2008. The metabolic balance at two contrasting sites in the Southern
929 Ocean: The iron-fertilized Kerguelen area and HNLC waters. *Deep Sea Res. Part II Top. Stud.*
930 *Oceanogr.*, *KEOPS: Kerguelen Ocean and Plateau compared Study* 55, 766–776.
931 doi:10.1016/j.dsr2.2007.12.006

932 Le Moigne, F.A.C., Sanders, R.J., Villa-Alfageme, M., Martin, A.P., Pabortsava, K., Planquette, H., Morris, P.J.,
933 Thomalla, S.J., 2012. On the proportion of ballast versus non-ballast associated carbon export in the
934 surface ocean. *Geophys. Res. Lett.* 39, L15610. doi:10.1029/2012GL052980

935 Lenton, A., Tilbrook, B., Law, R.M., Bakker, D., Doney, S.C., Gruber, N., Ishii, M., Hoppema, M., Lovenduski,
936 N.S., Matear, R.J., McNeil, B.I., Metzl, N., Mikaloff Fletcher, S.E., Monteiro, P.M.S., Rödenbeck, C.,
937 Sweeney, C., Takahashi, T., 2013. Sea–air CO₂ fluxes in the Southern Ocean for the period 1990–2009.
938 *Biogeosciences* 10, 4037–4054. doi:10.5194/bg-10-4037-2013

939 Le Quéré, C., Andres, R.J., Boden, T., Conway, T., Houghton, R.A., House, J.I., Marland, G., Peters, G.P., van
940 der Werf, G.R., Ahlström, A., Andrew, R.M., Bopp, L., Canadell, J.G., Ciais, P., Doney, S.C., Enright,
941 C., Friedlingstein, P., Huntingford, C., Jain, A.K., Jourdain, C., Kato, E., Keeling, R.F., Klein
942 Goldewijk, K., Levis, S., Levy, P., Lomas, M., Poulter, B., Raupach, M.R., Schwinger, J., Sitch, S.,
943 Stocker, B.D., Viovy, N., Zaehle, S., Zeng, N., 2013. The global carbon budget 1959–2011. *Earth Syst.*
944 *Sci. Data* 5, 165–185. doi:10.5194/essd-5-165-2013

945 Levy, M., Bopp, L., Karleskind, P., Resplandy, L., Ethe, C., Pinsard, F., 2013. Physical pathways for carbon
946 transfers between the surface mixed layer and the ocean interior. *Glob. Biogeochem. Cycles* 27, 1001–
947 1012. doi:10.1002/gbc.20092

948 Lima, I.D., Lam, P.J., Doney, S.C., 2014a. Dynamics of particulate organic carbon flux in a global ocean model.
949 *Biogeosciences* 11, 1177–1198. doi:10.5194/bg-11-1177-2014

950 Lima, I.D., Lam, P.J., Doney, S.C., 2014b. Dynamics of particulate organic carbon flux in a global ocean model.
951 *Biogeosciences* 11, 1177–1198. doi:10.5194/bg-11-1177-2014

952 Lutz, M.J., Caldeira, K., Dunbar, R.B., Behrenfeld, M.J., 2007. Seasonal rhythms of net primary production and
953 particulate organic carbon flux to depth describe the efficiency of biological pump in the global ocean.
954 *J. Geophys. Res. Oceans* 112, C10011. doi:10.1029/2006JC003706

955 Maiti, K., Charette, M.A., Buesseler, K.O., Kahru, M., 2013. An inverse relationship between production and
956 export efficiency in the Southern Ocean. *Geophys. Res. Lett.* 40, 1557–1561. doi:10.1002/grl.50219

957 Manno, C., Stowasser, G., Enderlein, P., Fielding, S., Tarling, G.A., 2014. The contribution of zooplankton
958 faecal pellets to deep carbon transport in the Scotia Sea (Southern Ocean). *Biogeosciences Discuss* 11,
959 16105–16134. doi:10.5194/bgd-11-16105-2014

960 Maraldi, C., Lyard, F., Testut, L., Coleman, R., 2011. Energetics of internal tides around the Kerguelen Plateau
961 from modeling and altimetry. *J. Geophys. Res. Oceans* 116, C06004. doi:10.1029/2010JC006515

962 Maraldi, C., Mongin, M., Coleman, R., Testut, L., 2009. The influence of lateral mixing on a phytoplankton
963 bloom: Distribution in the Kerguelen Plateau region. *Deep Sea Res. Part Oceanogr. Res. Pap.* 56, 963–
964 973. doi:10.1016/j.dsr.2008.12.018

965 Maritorena, S., Siegel, D.A., 2005. Consistent merging of satellite ocean color data sets using a bio-optical
966 model. *Remote Sens. Environ.* 94, 429–440. doi:10.1016/j.rse.2004.08.014

967 Martin, J.H., Knauer, G.A., Karl, D.M., Broenkow, W.W., 1987. VERTEX: carbon cycling in the northeast
968 Pacific. *Deep Sea Res. Part Oceanogr. Res. Pap.* 34, 267–285. doi:10.1016/0198-0149(87)90086-0

969 Martin, P., van der Loeff, M.R., Cassar, N., Vandromme, P., d' Ovidio, F., Stemmann, L., Rengarajan, R.,
970 Soares, M., González, H.E., Ebersbach, F., Lampitt, R.S., Sanders, R., Barnett, B.A., Smetacek, V.,
971 Naqvi, S.W.A., 2013. Iron fertilization enhanced net community production but not downward particle
972 flux during the Southern Ocean iron fertilization experiment LOHAFEX. *Glob. Biogeochem. Cycles*
973 27, 871–881. doi:10.1002/gbc.20077

974 Matsuno, K., Yamaguchi, A., Fujiwara, A., Onodera, J., Watanabe, E., Imai, I., Chiba, S., Harada, N., Kikuchi,
975 T., 2014. Seasonal changes in mesozooplankton swimmers collected by sediment trap moored at a

976 single station on the Northwind Abyssal Plain in the western Arctic Ocean. *J. Plankton Res.* 36, 490–
977 502. doi:10.1093/plankt/fbt092

978 McLeod, D.J., Hosie, G.W., Kitchener, J.A., Takahashi, K.T., Hunt, B.P.V., 2010. Zooplankton Atlas of the
979 Southern Ocean: The SCAR SO-CPR Survey (1991–2008). *Polar Sci., Antarctic Biology in the 21st*
980 *Century - Advances in and beyond IPY 4*, 353–385. doi:10.1016/j.polar.2010.03.004

981 Measures, C.I., Brown, M.T., Selph, K.E., Apprill, A., Zhou, M., Hatta, M., Hiscock, W.T., 2013. The influence
982 of shelf processes in delivering dissolved iron to the HNLC waters of the Drake Passage, Antarctica.
983 *Deep Sea Res. Part II Top. Stud. Oceanogr.* 90, 77–88. doi:10.1016/j.dsr2.2012.11.004

984 Metzl, N., Brunet, C., Jabaud-Jan, A., Poisson, A., Schauer, B., 2006. Summer and winter air–sea CO₂ fluxes in
985 the Southern Ocean. *Deep Sea Res. Part Oceanogr. Res. Pap.* 53, 1548–1563.
986 doi:10.1016/j.dsr.2006.07.006

987 Moore, J.K., Doney, S.C., Lindsay, K., 2004. Upper ocean ecosystem dynamics and iron cycling in a global
988 three-dimensional model. *Glob. Biogeochem. Cycles* 18, GB4028. doi:10.1029/2004GB002220

989 Morales, C.E., 1987. Carbon and nitrogen content of copepod faecal pellets: effect of food concentration and
990 feeding behaviour. *Mar. Ecol. Prog. Ser.* 36, 107–114.

991 Obernosterer, I., Christaki, U., Lefèvre, D., Catala, P., Van Wambeke, F., Lebaron, P., 2008. Rapid bacterial
992 mineralization of organic carbon produced during a phytoplankton bloom induced by natural iron
993 fertilization in the Southern Ocean. *Deep Sea Res. Part II Top. Stud. Oceanogr.* 55, 777–789.
994 doi:10.1016/j.dsr2.2007.12.005

995 O’Neill, L.P., Benitez-Nelson, C.R., Styles, R.M., Tappa, E., Thunell, R.C., 2005. Diagenetic effects on
996 particulate phosphorus samples collected using formalin poisoned sediment traps. *Limnol. Oceanogr.*
997 *Methods* 3, 308–317. doi:10.4319/lom.2005.3.308

998 Park, Y.-H., Charriaud, E., Pino, D.R., Jeandel, C., 1998. Seasonal and interannual variability of the mixed layer
999 properties and steric height at station KERFIX, southwest of Kerguelen. *J. Mar. Syst.* 17, 571–586.
1000 doi:10.1016/S0924-7963(98)00065-7

1001 Park, Y.-H., Fuda, J.-L., Durand, I., Naveira Garabato, A.C., 2008a. Internal tides and vertical mixing over the
1002 Kerguelen Plateau. *Deep Sea Res. Part II Top. Stud. Oceanogr.* 55, 582–593.
1003 doi:10.1016/j.dsr2.2007.12.027

1004 Park, Y.-H., Roquet, F., Durand, I., Fuda, J.-L., 2008b. Large-scale circulation over and around the Northern
1005 Kerguelen Plateau. *Deep Sea Res. Part II Top. Stud. Oceanogr.* 55, 566–581.
1006 doi:10.1016/j.dsr2.2007.12.030

1007 Peterson, M.L., Wakeham, S.G., Lee, C., Askea, M.A., Miquel, J.C., 2005. Novel techniques for collection of
1008 sinking particles in the ocean and determining their settling rates. *Limnol. Oceanogr. Methods* 3, 520–
1009 532. doi:10.4319/lom.2005.3.520

1010 Picheral, M., Guidi, L., Stemmann, L., Karl, D.M., Iddaoud, G., Gorsky, G., 2010. The Underwater Vision
1011 Profiler 5: An advanced instrument for high spatial resolution studies of particle size spectra and
1012 zooplankton. *Limnol. Oceanogr. Methods* 8, 462–473. doi:10.4319/lom.2010.8.462

1013 Pinkerton, M.H., Smith, A.N.H., Raymond, B., Hosie, G.W., Sharp, B., Leathwick, J.R., Bradford-Grieve, J.M.,
1014 2010. Spatial and seasonal distribution of adult *Oithona similis* in the Southern Ocean: Predictions
1015 using boosted regression trees. *Deep Sea Res. Part Oceanogr. Res. Pap.* 57, 469–485.
1016 doi:10.1016/j.dsr.2009.12.010

1017 Planchon, F., Ballas, D., Cavagna, A.-J., Bowie, A.R., Davies, D., Trull, T., Laurenceau, E., Van Der Merwe, P.,
1018 Dehairs, F., 2014. Carbon export in the naturally iron-fertilized Kerguelen area of the Southern Ocean
1019 based on the 234Th approach. *Biogeosciences Discuss* 11, 15991–16032. doi:10.5194/bgd-11-15991-
1020 2014

1021 Pollard, R., Sanders, R., Lucas, M., Statham, P., 2007. The Crozet Natural Iron Bloom and Export Experiment
1022 (CROZEX). *Deep Sea Res. Part II Top. Stud. Oceanogr.* 54, 1905–1914.
1023 doi:10.1016/j.dsr2.2007.07.023

1024 Pollard, R.T., Salter, I., Sanders, R.J., Lucas, M.I., Moore, C.M., Mills, R.A., Statham, P.J., Allen, J.T., Baker,
1025 A.R., Bakker, D.C.E., Charette, M.A., Fielding, S., Fones, G.R., French, M., Hickman, A.E., Holland,
1026 R.J., Hughes, J.A., Jickells, T.D., Lampitt, R.S., Morris, P.J., Nédélec, F.H., Nielsdóttir, M., Planquette,
1027 H., Popova, E.E., Poulton, A.J., Read, J.F., Seeyave, S., Smith, T., Stinchcombe, M., Taylor, S.,
1028 Thomalla, S., Venables, H.J., Williamson, R., Zubkov, M.V., 2009. Southern Ocean deep-water carbon
1029 export enhanced by natural iron fertilization. *Nature* 457, 577–580. doi:10.1038/nature07716

1030 Redfield, A., 1934. On the proportions of organic derivatives in sea water and their relation to the composition of
1031 plankton. *James Johnstone Meml. Vol. Univ. Press Liverpool.* 177–192.

1032 Rembauville, M., Blain, S., Armand, L., Quéguiner, B., Salter, I., 2014. Export fluxes in a naturally fertilized
1033 area of the Southern Ocean, the Kerguelen Plateau: ecological vectors of carbon and biogenic silica to
1034 depth (Part 2). *Biogeosciences Discuss* 11, 17089–17150. doi:10.5194/bgd-11-17089-2014

1035 Rigual-Hernández, A.S., Trull, T.W., Bray, S.G., Closset, I., Armand, L.K., 2015. Seasonal dynamics in diatom
1036 and particulate export fluxes to the deep sea in the Australian sector of the southern Antarctic Zone. *J.*
1037 *Mar. Syst.* 142, 62–74. doi:10.1016/j.jmarsys.2014.10.002

1038 Rivkin, R.B., Legendre, L., 2001. Biogenic carbon cycling in the upper ocean: effects of microbial respiration.
1039 *Science* 291, 2398–2400. doi:10.1126/science.291.5512.2398

1040 Rynearson, T.A., Richardson, K., Lampitt, R.S., Sieracki, M.E., Poulton, A.J., Lyngsgaard, M.M., Perry, M.J.,
1041 2013. Major contribution of diatom resting spores to vertical flux in the sub-polar North Atlantic. *Deep*
1042 *Sea Res. Part Oceanogr. Res. Pap.* 82, 60–71. doi:10.1016/j.dsr.2013.07.013

1043 Saba, G.K., Steinberg, D.K., 2012. Abundance, Composition, and Sinking Rates of Fish Fecal Pellets in the
1044 Santa Barbara Channel. *Sci. Rep.* 2. doi:10.1038/srep00716

1045 Salter, I., Kemp, A.E.S., Lampitt, R.S., Gledhill, M., 2010. The association between biogenic and inorganic
1046 minerals and the amino acid composition of settling particles. *Limnol. Oceanogr.* 55, 2207–2218.
1047 doi:10.4319/lo.2010.55.5.2207

1048 Salter, I., Kemp, A.E.S., Moore, C.M., Lampitt, R.S., Wolff, G.A., Holtvoeth, J., 2012. Diatom resting spore
1049 ecology drives enhanced carbon export from a naturally iron-fertilized bloom in the Southern Ocean.
1050 *Glob. Biogeochem. Cycles* 26, GB1014. doi:10.1029/2010GB003977

1051 Salter, I., Lampitt, R.S., Sanders, R., Poulton, A., Kemp, A.E.S., Boorman, B., Saw, K., Pearce, R., 2007.
1052 Estimating carbon, silica and diatom export from a naturally fertilised phytoplankton bloom in the
1053 Southern Ocean using PELAGRA: A novel drifting sediment trap. *Deep Sea Res. Part II Top. Stud.*
1054 *Oceanogr., The Crozet Natural Iron Bloom and Export Experiment CROZEX* 54, 2233–2259.
1055 doi:10.1016/j.dsr2.2007.06.008

1056 Salter, I., Schiebel, R., Ziveri, P., Movellan, A., Lampitt, R., Wolff, G.A., 2014. Carbonate counter pump
1057 stimulated by natural iron fertilization in the Polar Frontal Zone. *Nat. Geosci.* 7, 885–889.
1058 doi:10.1038/ngeo2285

1059 Sarmiento, J.L., Gruber, N., 2006. *Ocean Biogeochemical Dynamics*. Princeton University Press, Princeton.

1060 Sarmiento, J.L., Le Quééré, C., 1996. Oceanic Carbon Dioxide Uptake in a Model of Century-Scale Global
1061 Warming. *Science* 274, 1346–1350.

1062 Sarthou, G., Timmermans, K.R., Blain, S., Tréguer, P., 2005. Growth physiology and fate of diatoms in the
1063 ocean: a review. *J. Sea Res., Iron Resources and Oceanic Nutrients - Advancement of Global*
1064 *Environmental Simulations* 53, 25–42. doi:10.1016/j.seares.2004.01.007

1065 Savoye, N., Benitez-Nelson, C., Burd, A.B., Cochran, J.K., Charette, M., Buesseler, K.O., Jackson, G.A., Roy-
1066 Barman, M., Schmidt, S., Elskens, M., 2006. ²³⁴Th sorption and export models in the water column: A
1067 review. *Mar. Chem., Future Applications of ²³⁴Th in Aquatic Ecosystems (FATE)* 100, 234–249.
1068 doi:10.1016/j.marchem.2005.10.014

1069 Savoye, N., Trull, T.W., Jacquet, S.H.M., Navez, J., Dehairs, F., 2008. ²³⁴Th-based export fluxes during a
1070 natural iron fertilization experiment in the Southern Ocean (KEOPS). *Deep Sea Res. Part II Top. Stud.*
1071 *Oceanogr., KEOPS: Kerguelen Ocean and Plateau compared Study* 55, 841–855.
1072 doi:10.1016/j.dsr2.2007.12.036

1073 Schlitzer, R., 2004. Export production in the Equatorial and North Pacific derived from dissolved oxygen,
1074 nutrient and carbon data. *J. Oceanogr. Vol 60 No 1 Pp* 53–62.

1075 Schulz, M., Mudelsee, M., 2002. REDFIT: estimating red-noise spectra directly from unevenly spaced
1076 paleoclimatic time series. *Comput. Geosci.* 28, 421–426. doi:10.1016/S0098-3004(01)00044-9

1077 Seeyave, S., Lucas, M.I., Moore, C.M., Poulton, A.J., 2007. Phytoplankton productivity and community
1078 structure in the vicinity of the Crozet Plateau during austral summer 2004/2005. *Deep Sea Res. Part II*
1079 *Top. Stud. Oceanogr., The Crozet Natural Iron Bloom and Export Experiment CROZEX* 54, 2020–
1080 2044. doi:10.1016/j.dsr2.2007.06.010

1081 Smetacek, V., Assmy, P., Henjes, J., 2004. The role of grazing in structuring Southern Ocean pelagic ecosystems
1082 and biogeochemical cycles. *Antarct. Sci.* 16, 541–558. doi:10.1017/S0954102004002317

1083 Tarling, G.A., Ward, P., Atkinson, A., Collins, M.A., Murphy, E.J., 2012. DISCOVERY 2010: Spatial and
1084 temporal variability in a dynamic polar ecosystem. *Deep Sea Res. Part II Top. Stud. Oceanogr.* 59–60,
1085 1–13. doi:10.1016/j.dsr2.2011.10.001

1086 Thomalla, S.J., Fauchereau, N., Swart, S., Monteiro, P.M.S., 2011. Regional scale characteristics of the seasonal
1087 cycle of chlorophyll in the Southern Ocean. *Biogeosciences* 8, 2849–2866. doi:10.5194/bg-8-2849-
1088 2011

1089 Trull, T.W., Bray, S.G., Buesseler, K.O., Lamborg, C.H., Manganini, S., Moy, C., Valdes, J., 2008. In situ
1090 measurement of mesopelagic particle sinking rates and the control of carbon transfer to the ocean
1091 interior during the Vertical Flux in the Global Ocean (VERTIGO) voyages in the North Pacific. *Deep*
1092 *Sea Res. Part II Top. Stud. Oceanogr.* 55, 1684–1695. doi:10.1016/j.dsr2.2008.04.021

1093 Trull, T.W., Davies, D., Casciotti, K., 2008. Insights into nutrient assimilation and export in naturally iron-
1094 fertilized waters of the Southern Ocean from nitrogen, carbon and oxygen isotopes. *Deep Sea Res. Part*
1095 *II Top. Stud. Oceanogr.* 55, 820–840. doi:10.1016/j.dsr2.2007.12.035

1096 Tsuda, A., Takeda, S., Saito, H., Nishioka, J., Kudo, I., Nojiri, Y., Suzuki, K., Uematsu, M., Wells, M.L.,
1097 Tsumune, D., Yoshimura, T., Aono, T., Aramaki, T., Cochlan, W.P., Hayakawa, M., Imai, K., Isada, T.,
1098 Iwamoto, Y., Johnson, W.K., Kameyama, S., Kato, S., Kiyosawa, H., Kondo, Y., Levasseur, M.,
1099 Machida, R.J., Nagao, I., Nakagawa, F., Nakanishi, T., Nakatsuka, S., Narita, A., Noiri, Y., Obata, H.,
1100 Ogawa, H., Oguma, K., Ono, T., Sakuragi, T., Sasakawa, M., Sato, M., Shimamoto, A., Takata, H.,
1101 Trick, C.G., Watanabe, Y.W., Wong, C.S., Yoshie, N., 2007. Evidence for the grazing hypothesis:
1102 Grazing reduces phytoplankton responses of the HNLC ecosystem to iron enrichment in the western
1103 subarctic pacific (SEEDS II). *J. Oceanogr.* 63, 983–994. doi:10.1007/s10872-007-0082-x

1104 Turner, J.T., 2002. Zooplankton fecal pellets, marine snow and sinking phytoplankton blooms. *Aquat. Microb.*
1105 *Ecol.* 27, 57–102. doi:10.3354/ame027057

1106 Uitz, J., Claustre, H., Griffiths, F.B., Ras, J., Garcia, N., Sandroni, V., 2009. A phytoplankton class-specific
1107 primary production model applied to the Kerguelen Islands region (Southern Ocean). *Deep Sea Res.*
1108 *Part Oceanogr. Res. Pap.* 56, 541–560. doi:10.1016/j.dsr.2008.11.006

1109 Villareal, T.A., Adornato, L., Wilson, C., Schoenbaechler, C.A., 2011. Summer blooms of diatom-diazotroph
1110 assemblages and surface chlorophyll in the North Pacific gyre: A disconnect. *J. Geophys. Res. Oceans*
1111 116, C03001. doi:10.1029/2010JC006268

1112 Volk, T., Hoffert, M.I., 1985. Ocean carbon pumps: Analysis of relative strengths and efficiencies in ocean-
1113 driven atmospheric CO₂ changes, in: Sundquist, E.T., Broecker, W.S. (Eds.), *Geophysical Monograph*
1114 *Series.* American Geophysical Union, Washington, D. C., pp. 99–110.

1115
1116

1117 **Table 1:** Dynamics of carbon and nitrogen export fluxes at station A3 collected by the
 1118 sediment trap at 289 m.

Cup	Start	Stop	Fluxes ($\text{mmol m}^{-2} \text{d}^{-1}$)			Contribution to annual export (%)	
			POC	PON	POC:PON	POC	PON
1	21/10/2011	04/11/2011	0.15±0.01	0.02±0.00	6.80±0.56	2.11±0.06	2.30±0.01
2	04/11/2011	18/11/2011	0.14 ±0.01	0.02±0.00	6.09±0.67	1.94±0.16	2.27±0.15
3	18/11/2011	02/12/2011	0.15±0.01	0.02±0.00	7.33±0.31	2.12±0.06	1.99±0.06
4	02/12/2011	12/12/2011	1.60±0.04	0.23±0.01	6.95±0.29	16.18±0.45	16.48±0.07
5	12/12/2011	22/12/2011	0.34±0.00	0.05±0.00	6.87±0.08	3.41±0.03	3.64±0.03
6	22/12/2011	01/01/2012	0.51±0.04	0.08±0.01	6.70±0.78	4.82±0.76	5.50±0.39
7	01/01/2012	11/01/2012	0.42±0.02	0.06±0.00	6.73±0.46	4.23±0.14	4.65±0.42
8	11/01/2012	25/01/2012	0.34±0.01	0.05±0.00	6.94±0.38	4.83±0.18	4.84±0.11
9	25/01/2012	08/02/2012	1.47±0.03	0.20±0.01	7.38±0.26	20.98±0.57	21.07±0.05
10	08/02/2012	22/02/2012	0.55±0.04	0.08±0.00	6.97±0.88	7.83±0.64	8.36±0.57
11	22/02/2012	31/05/2012	0.27±0.01	0.03±0.00	8.09±0.22	26.84±0.47	24.12±0.20
12	31/05/2012	07/09/2012	0.04±0.00	0.01±0.00	6.06±0.17	4.71±0.90	4.78±0.09
Annual export ($\text{mmol m}^{-2} \text{y}^{-1}$)			98.24±4.35	13.59±0.30			

1119

1120

1121 **Table 2:** Number of swimmer individuals found in each cup and swimmer intrusion rate
 1122 (number d⁻¹, *bold italic* numbers) for each taxa and for the total swimmers.

Cup	Copepod	Pteropod	Euphausi d	Ostracod	Amphipo d	Cnidaria n	Polychaet e	Ctenopho re	Siphonop hore	Salp	Total
1	166	13	1	2	1	0	0	0	0	0	183
	<i>12</i>	<i>1</i>	<i><1</i>	<i><1</i>	<i><1</i>	<i>0</i>	<i>0</i>	<i>0</i>	<i>0</i>	<i>0</i>	<i>13</i>
2	55	0	0	0	0	0	0	0	0	0	55
	<i>4</i>	<i>0</i>	<i>0</i>	<i>0</i>	<i>0</i>	<i>0</i>	<i>0</i>	<i>0</i>	<i>0</i>	<i>0</i>	<i>4</i>
3	0	0	0	0	0	0	0	0	0	0	0
	<i>0</i>	<i>0</i>	<i>0</i>	<i>0</i>	<i>0</i>	<i>0</i>	<i>0</i>	<i>0</i>	<i>0</i>	<i>0</i>	<i>0</i>
4	113	0	0	0	0	0	0	0	0	0	113
	<i>11</i>	<i>0</i>	<i>0</i>	<i>0</i>	<i>0</i>	<i>0</i>	<i>0</i>	<i>0</i>	<i>0</i>	<i>0</i>	<i>11</i>
5	0	0	0	0	0	0	0	0	0	0	0
	<i>0</i>	<i>0</i>	<i>0</i>	<i>0</i>	<i>0</i>	<i>0</i>	<i>0</i>	<i>0</i>	<i>0</i>	<i>0</i>	<i>0</i>
6	540	0	1	0	2	5	1	4	1	0	554
	<i>54</i>	<i>0</i>	<i><1</i>	<i>0</i>	<i><1</i>	<i><1</i>	<i>0</i>	<i>0</i>	<i>0</i>	<i>0</i>	<i>55</i>
7	583	0	0	0	0	2	2	3	0	0	590
	<i>58</i>	<i>0</i>	<i>0</i>	<i>0</i>	<i>0</i>	<i><1</i>	<i><1</i>	<i><1</i>	<i>0</i>	<i>0</i>	<i>58</i>
8	686	33	2	2	8	5	1	4	0	0	741
	<i>49</i>	<i>2</i>	<i><1</i>	<i><1</i>	<i>1</i>	<i><1</i>	<i><1</i>	<i><1</i>	<i>0</i>	<i>0</i>	<i>52</i>
9	392	14	4	3	121	4	2	0	0	0	540
	<i>28</i>	<i>1</i>	<i><1</i>	<i><1</i>	<i>9</i>	<i><1</i>	<i><1</i>	<i>0</i>	<i>0</i>	<i>0</i>	<i>38</i>
10	264	69	1	2	18	11	0	2	0	0	367
	<i>19</i>	<i>5</i>	<i><1</i>	<i><1</i>	<i>1</i>	<i>1</i>	<i>0</i>	<i><1</i>	<i>0</i>	<i>0</i>	<i>26</i>
11	54	0	0	0	29	4	1	0	0	0	88
	<i>1</i>	<i>0</i>	<i>0</i>	<i>0</i>	<i><1</i>	<i><1</i>	<i><1</i>	<i>0</i>	<i>0</i>	<i>0</i>	<i>1</i>
12	1481	44	5	7	2	3	2	0	0	1	1544
	<i>15</i>	<i><1</i>	<i><1</i>	<i><1</i>	<i><1</i>	<i><1</i>	<i><1</i>	<i>0</i>	<i>0</i>	<i><1</i>	<i>15</i>

1123

1124

1125 **Table 3:** Synthesis of estimates of POC fluxes at the base of, or under, the mixed layer at
 1126 station A3 from the KEOPS 1 cruise.

Author	Method	Period	Depth (m)	POC flux ($\text{mmol m}^{-2} \text{d}^{-1}$)	
KEOPS1					
Savoie et al., 2008	^{234}Th deficit	23 Jan – 12 Feb 2005	100	23 ± 3.6	
			150	25.7 ± 3.6	
			200	24.5 ± 6.8	
Ebersbach and Trull, 2008	Drifting gel trap, optical measurements and constant C conversion factor	4 Feb 2005	200	23.9	
			100	5.3	
		12 Feb 2005	200	5.2	
			330	0.7	
			430	1	
Jouandet et al., 2008	Annual DIC budget	Annual	MLD base	85	
Trull et al., 2008b	Drifting sediment trap	4 Feb 2005	200	7.3-10	
		12 Feb 2005		3-3.1	
Jouandet et al., 2011	In situ optical measurement (UVP) and power function C conversion factor	22 Jan 2005	200	72.4	
			330	27.2	
			400	21.6	
		23 Jan 2005	200	29.8	
			330	26.8	
			400	15.9	
		12 Feb 2005	200	4.8	
			330	5.6	
			400	7.9	
KEOPS2					
Planchon et al., 2014	^{234}Th deficit, steady state model	20 Oct 2011	100	3.5 ± 0.9	
			150	3.9 ± 0.9	
			200	3.7 ± 0.9	
		16 Nov 2011	100	4.6 ± 1.5	
			150	7.1 ± 1.5	
			200	3.1 ± 0.6	
		16 Nov 2011	^{234}Th deficit, non steady state model	100	7.3 ± 1.8
				150	8.4 ± 1.8
				200	3.8 ± 0.8
Laurenceau et al., 2014	Drifting gel trap, optical measurement of particles	16 Nov 2011	210	5.5	
			210	2.2	
Jouandet et al., 2014	In situ optical measurement (UVP) and power function C conversion factor	21 Oct 2011	200	0.2	
			350	0.1	
		16 Nov 2011	200	1.9	
350	0.3				

1128 **Figures captions**

1129 **Figure 1.** Localization of the Kerguelen Plateau in the Indian sector of the Southern Ocean
1130 and detailed map of the satellite-derived surface chlorophyll *a* concentration (MODIS level 3
1131 product) averaged over the sediment trap deployment period. Sediment trap location at the A3
1132 station is represented by a black dot, whereas the black circle represents the 100 km radius
1133 area used to average the surface chlorophyll *a* time series. Arrows represent surface
1134 geostrophic circulation derived from the absolute dynamic topography (AVISO product).
1135 Positions of the Antarctic Circumpolar Current core (AAC core), the Polar Front (PF) and the
1136 Fawn Through Current (FTC) are shown by thick black arrows. Grey lines are 500 m and
1137 1000 m isobaths.

1138 **Figure 2.** Schematic of the instrumented mooring line against vertical temperature profiles.
1139 The sediment trap and the current meter/CTD sensor location on the mooring line are shown
1140 by white circles. Temperature profiles performed during the sediment trap deployment (20
1141 October 2011) are represented by grey lines. Black full line is the median temperature profile
1142 from 12 casts realized on the 16 November 2011. Dashed black lines are the first and third
1143 quartiles from these casts. The grey rectangle represents the Kerguelen Plateau seafloor. The
1144 different water masses are Antarctic Surface Water (AASW), Winter Water (WW) and Upper
1145 Circumpolar Deep Water (UCDW).

1146 **Figure 3.** Hydrological properties recorded by the instrument mooring at station A3. a) depth
1147 of the CTD sensor, b) salinity, c) potential temperature, d) line angle, e) current speed, grey
1148 lines are raw data, black lines are low-pass filtered data with a Gaussian filter (40 hour
1149 window as suggested by the spectral analysis), f) direction and speed of currents represented
1150 by vectors (under sampled with a 5 hours interval) and g) wind rose plot of current direction

1151 and intensities, dotted circles are directions relative frequencies and colors refer to current
1152 speed (m s^{-1}).

1153 **Figure 4.** Potential temperature/salinity diagram at station A3. Data are from the moored
1154 CTD (black dots), KEOPS1 (blue line) and KEOPS2 (red line). Grey lines are potential
1155 density anomaly. The different water masses are Antarctic Surface Water (AASW), Winter
1156 Water (WW) and Upper Circumpolar Deep Water (UCDW).

1157

1158 **Figure 5.** Power spectrum of the spectral analysis of a) depth time series and b) potential
1159 density anomaly time series. Pure red noise (null hypothesis) is represented by red dashed
1160 lines for each variable. The period corresponding to a significant power peak (power peak
1161 higher than the red noise) is written.

1162 **Figure 6.** Progressive vector diagram (integration of the current vectors all along the current
1163 meter record) calculated from current meter data at 319 m. The color scale refers to date.

1164 **Figure 7.** Seasonal variations of surface chlorophyll *a* and particulate organic carbon (POC)
1165 export. a) Seasonal surface chlorophyll concentration and 16 years climatology (Globcolour)
1166 averaged in a 100 km radius around the station A3 station ~~The black line represents the~~
1167 ~~climatology calculated for the period 1997/2013, whilst the green line corresponds to the~~
1168 ~~sediment trap deployment period (2011/2012). Error bars represent the inter annual standard~~
1169 ~~deviation for the climatology, and the spatial standard deviation for the 2011/2012 data.~~ b)
1170 POC flux (grey bars) and mass percentage of POC (red dotted line). Error bars are standard
1171 deviations from triplicates, bold italic numbers refer to cup number.

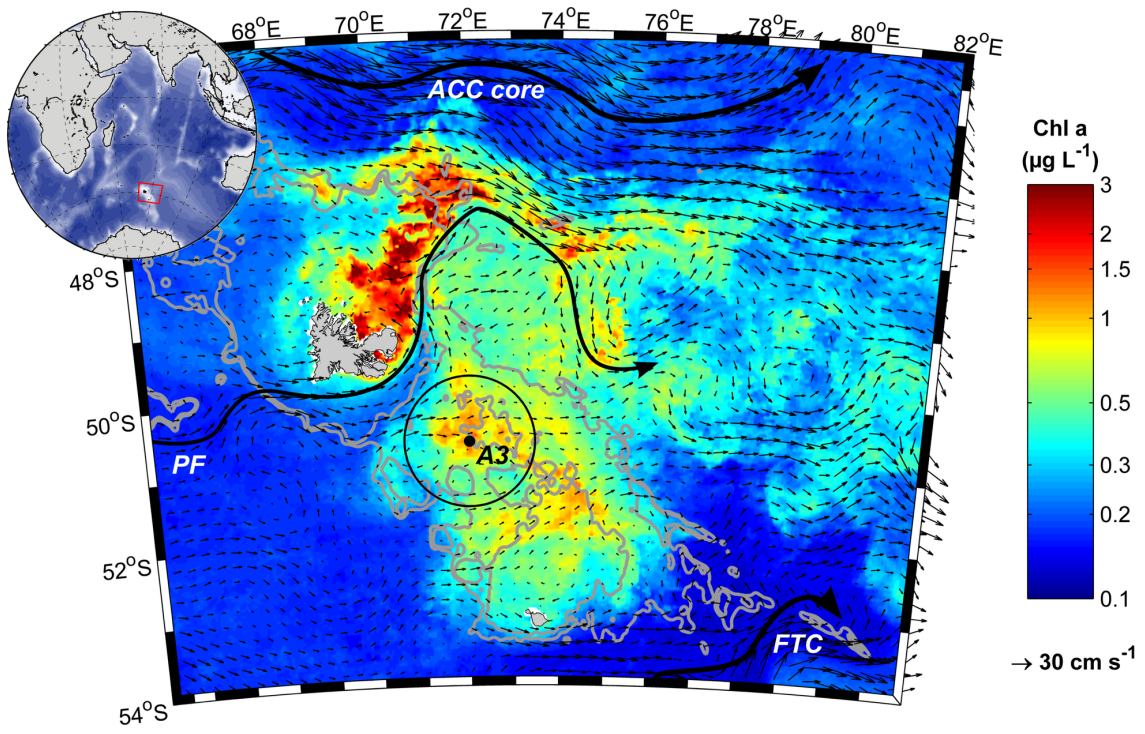


Figure 1.

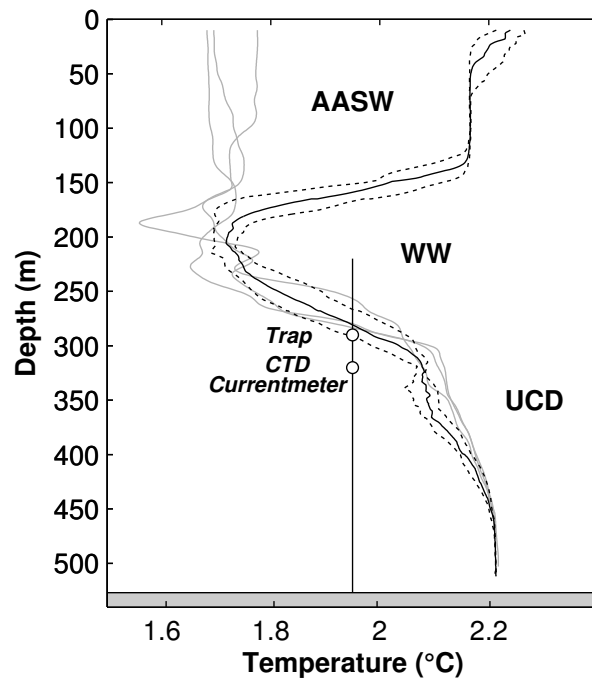


Figure 2.

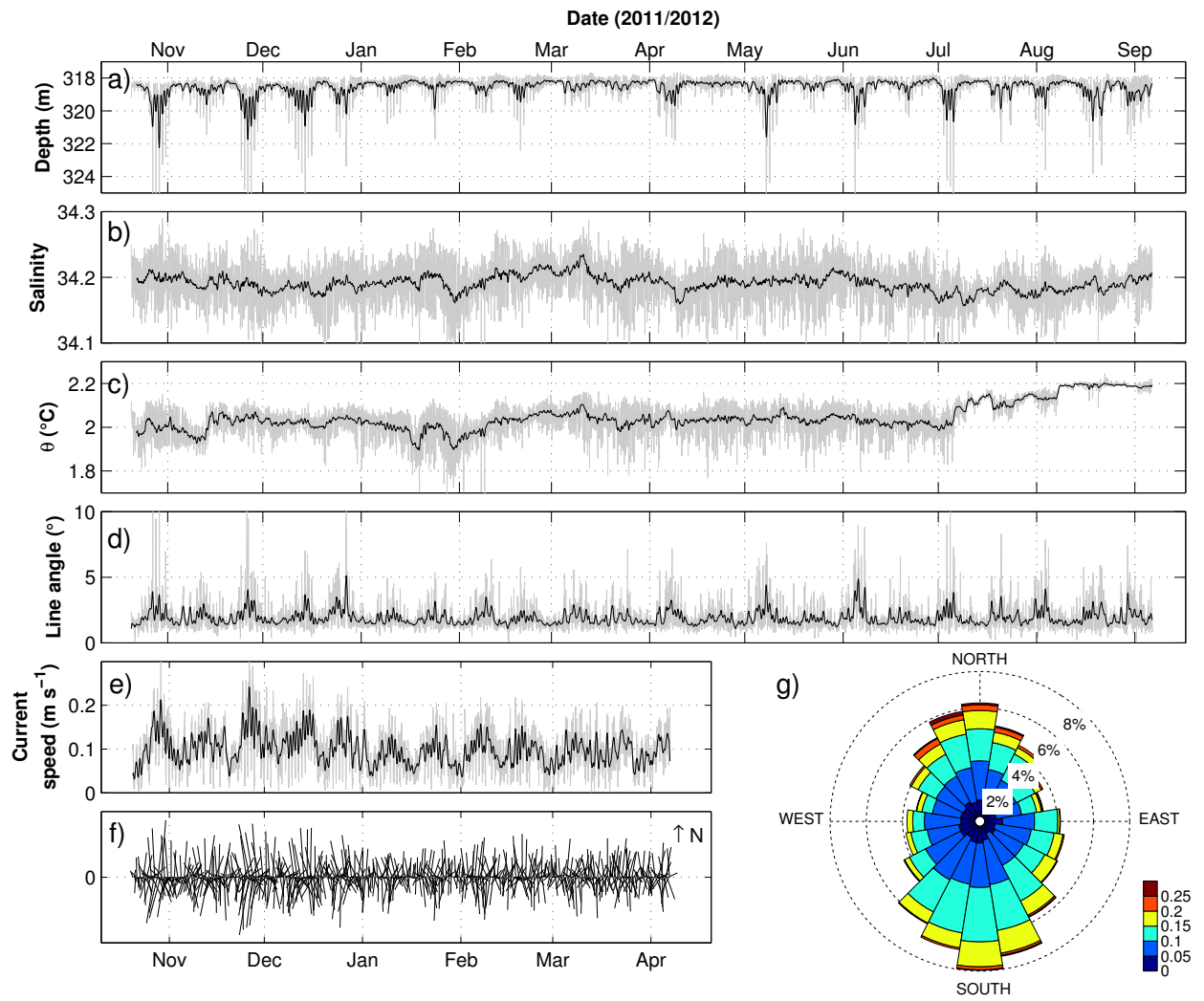


Figure 3.

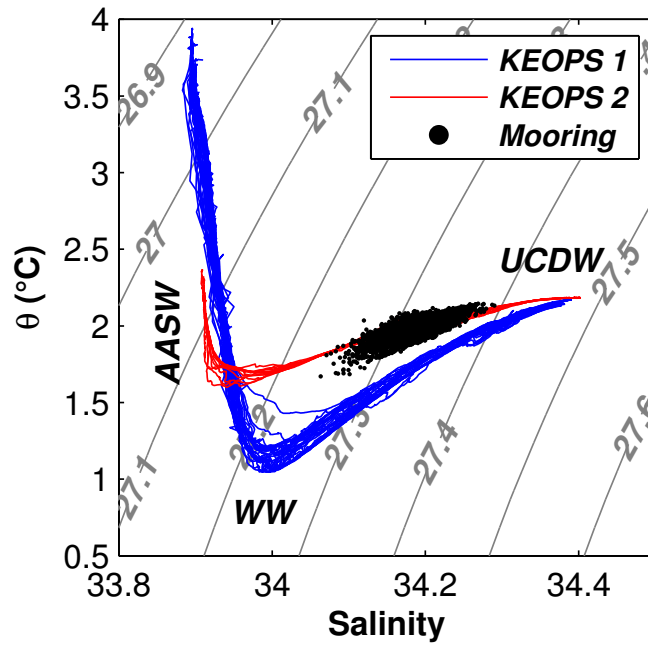


Figure 4.

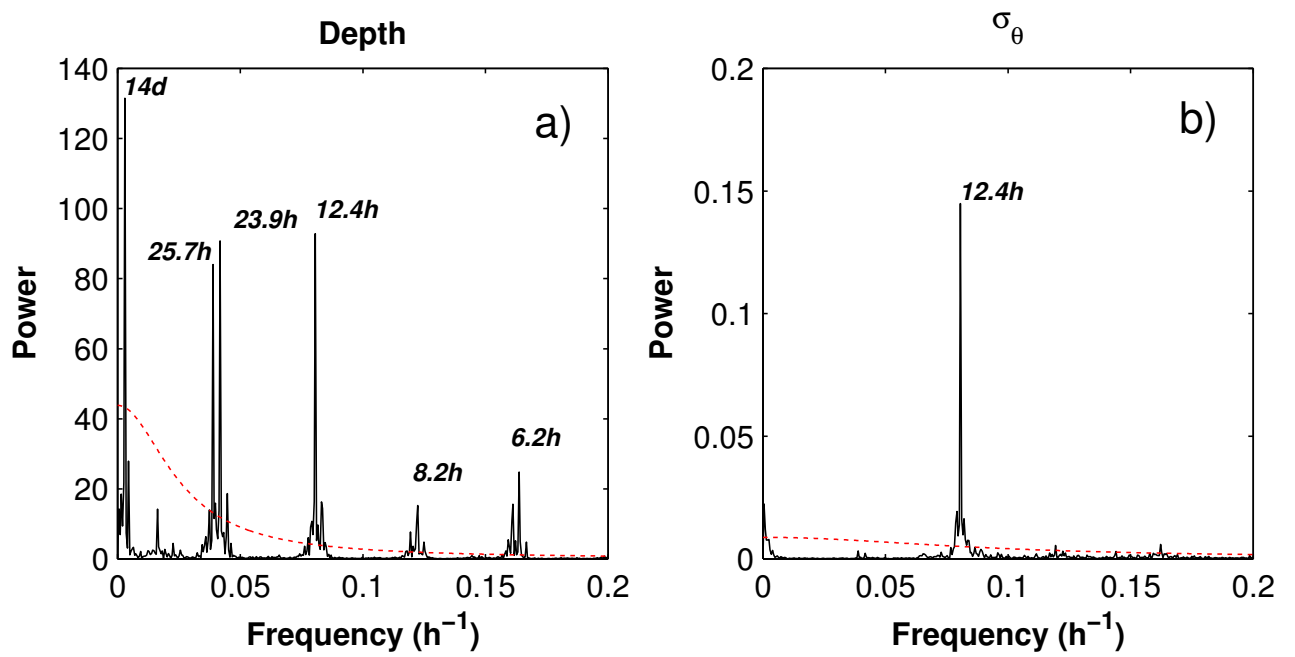


Figure 5.

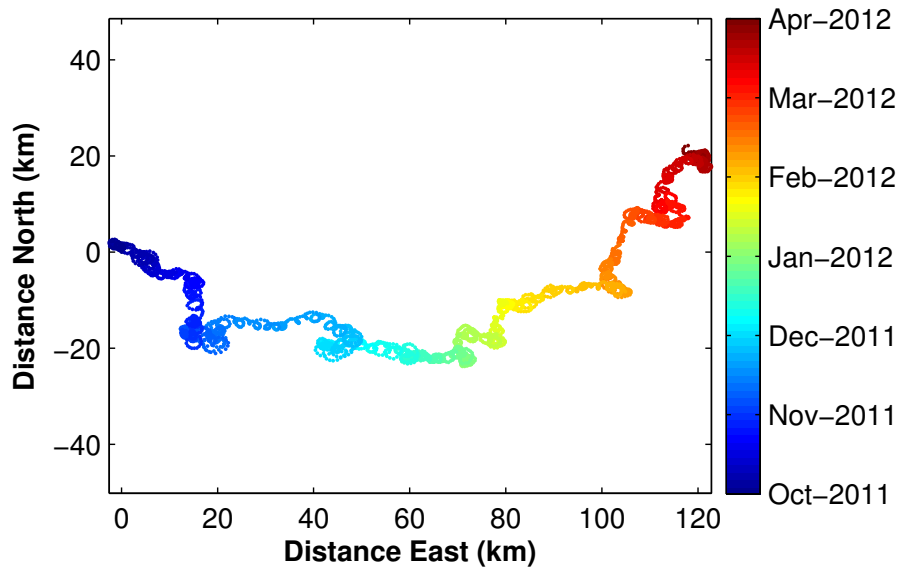


Figure 6.

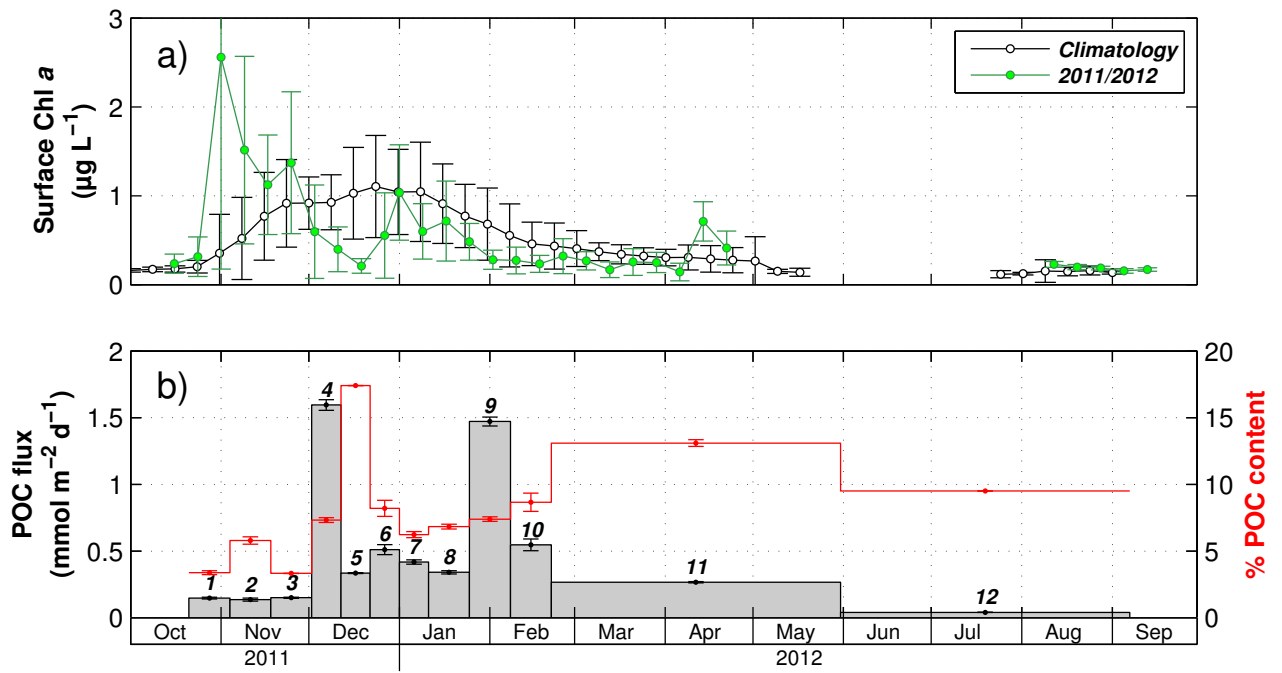


Figure 7.